
Theses and Dissertations

Spring 2017

Vibratory stimulation of thyroid epithelial mimics hormonal stimulation

Andrew P. Wagner
University of Iowa

Copyright © 2017 Andrew P. Wagner

This dissertation is available at Iowa Research Online: <http://ir.uiowa.edu/etd/5672>

Recommended Citation

Wagner, Andrew P. "Vibratory stimulation of thyroid epithelial mimics hormonal stimulation." PhD (Doctor of Philosophy) thesis, University of Iowa, 2017.
<http://ir.uiowa.edu/etd/5672>.

Follow this and additional works at: <http://ir.uiowa.edu/etd>



Part of the [Biomedical Engineering and Bioengineering Commons](#)

VIBRATORY STIMULATION OF THYROID EPITHELIAL MIMICS HORMONAL
STIMULATION

by

Andrew P. Wagner

A thesis submitted in partial fulfillment
of the requirements for the Doctor of Philosophy
degree in Biomedical Engineering in the
Graduate College of
The University of Iowa

May 2017

Thesis Supervisor: Assistant Professor Edward Sander
Professor Ingo Titze

Copyright by
Andrew P. Wagner
2017
All Rights Reserved

Graduate College
The University of Iowa
Iowa City, Iowa

CERTIFICATE OF APPROVAL

PH.D. THESIS

This is to certify that the Ph.D. thesis of

Andrew P. Wagner

has been approved by the Examining Committee for
the thesis requirement for the Doctor of Philosophy degree
in Biomedical Engineering at the May 2017 graduation.

Thesis Committee:

Edward Sander, Thesis Supervisor

Ingo Titze

Suresh Raghavan

Sarah Vigmostad

Henry Hoffman

ABSTRACT

Hypothyroidism is the most common endocrine disease, affecting approximately 4% of the population. Hypothyroidism is associated with a lack of energy and weight gain, as well as other complications that arise from hormone imbalance, including susceptibility to osteoporosis and heart disease. Hypothyroidism is characterized by a substantial decrease in thyroid hormone production that stems in part from a reduction in thyroid epithelial cell sensitivity to thyroid stimulating hormone (TSH), and the concomitant release of T₃ and T₄ hormones into the bloodstream. Recent work showing the importance of mechanical vibrations in maintaining physiological balance in other tissues and the close proximity of the thyroid gland to the vocal chords suggests that it may be possible to increase T₃ and T₄ release through vibrations/accelerations from vocalization. Therefore, the purpose of this study was to test the hypothesis that accelerations of thyroid epithelial cells *in vitro* at sonic frequencies can mimic a thyroid hormone response to TSH.

The first part of this dissertation has shown that vibration at physiological levels can stimulate thyroid hormone markers in thyroid epithelial cells. The second part of the dissertation suggests that increasing the vibration amplitudes and exposure time increases Fischer Rat Thyroid Line-5 cells response to vibration. The mechanism in which these cells sense the oscillational forces from the bioreactor were also investigated. Actin polymerization was shown to play a significant role in the thyroid epithelial cells ability to sense vibrations. These results may better help us understand how to use mechanical forces to help thyroid physiology.

PUBLIC ABSTRACT

Human vocalization has always been considered in the context of communication. In recent years, mechanical forces have been shown to have a wide variety of effects on biological systems. Since the vocal cords produce measurable vibrations to the surrounding tissue, including the thyroid, I hypothesize that vocalization could mechanically stimulate thyroid epithelial cells.

The data presented in this dissertation highlight some of the important factors for thyroid hormone synthesis. I was able to show that mechanical stimulation provided from vocalization has a similar response as hormonal stimulation on the thyroid. I also demonstrated that this response is dependent on the dosage of the oscillation.

Insight into thyroid stimulation via mechanical forces may be useful for a range of medical issues spanning from hypothyroidism to astronauts travelling in space.

TABLE OF CONTENTS

List of Tables	vii
List of Figures	viii
Chapter 1: Introduction.....	1
Motivation	1
Thyroid Anatomy and Physiology	2
Current Complication with Thyroid Health.....	4
Causes of Hypothyroidism	5
Complications from Hypothyroidism	6
Current Treatments	6
Gravitational Forces Acting on the Thyroid.....	8
Chapter 2: Test of Aim 1: Vibrational Forces Help Stimulate Thyroid Hormones.....	14
Introduction	14
Materials and Methods	16
Cell Culture.....	16
Application of Physiological Vibrations with a Torsional Rheometer-Bioreactor	17
Quantification of Metabolic Activity.....	19
Quantification of Cell Number	20
Quantification of Reactive Oxygen Species (ROS) Levels	20
Quantification of Cyclic Adenosine Monophosphate (cAMP) Levels.....	20
Thyroglobulin (TG) and Sodium/Iodine Symporter (NIS) Gene Expression Assessed with qPCR.....	21
Statistical Analysis	22
Results	23
Discussion.....	27
Chapter 3: Evaluate Aim 2: Cellular Cytoskeleton Plays an Important Role in Sensing Mechanical Forces	35
Introduction	35
Materials and Methods	37
Cell Culture.....	37
TRB Setup	38

Rho/ROCK Inhibition.....	38
Actin Polymerization Inhibition	39
Metabolic Activity Assay	39
Cell Number Quantification	40
Live/Dead	40
Statistical Analysis	40
Results	41
Discussion.....	45
Chapter 4: Develop New Vibration Bioreactor for a more Physiological Environment	47
Introduction	47
Material and Methods	47
Cell Culture.....	47
Voice Coil Bioreactor	48
Acceleration Measurement	49
Alamar Blue Assay	50
Quantification of Cell Number	50
Quantification of Reactive Oxygen Species (ROS) Levels	50
Statistical Analysis	51
Results	51
Discussion.....	59
Chapter 5: Evaluate Aim 3: Cellular Response to Vibratory Stimulation in a Dose Dependent Manner	62
Introduction	62
Material and Methods	63
Cell Culture.....	63
Voice Coil Bioreactor	64
Duty Cycle Analysis	64
Dosage Effects	64
Quantification of Metabolic Activity.....	65
Quantification of Cell Number	66
Quantification of Reactive Oxygen Species (ROS) Levels	66
Statistical Analysis	66
Results	67

Discussion and Conclusion.....	71
Chapter 6. Future Work and Discussion.....	74
Introduction	74
Material and Methods	75
Cell Culture.....	75
Application of Basement Membranes	76
Application of Vibrations with a Voice Coil Bioreactor	76
Quantification of Metabolic Activity.....	77
Quantification of Cell Number	77
Cell Morphology.....	78
Statistical Analysis	78
Results	78
Discussion and Conclusion.....	83
Appendix: Protocols	85
Media Preparation.....	85
Cyclic Adenosine Monophosphate (cAMP) Assay	86
DCF Protocol (Reactive Oxygen Detection)	87
Live Dead Protocol.....	87
Multiwell Disc and TRB Setup	88
REFERENCES	90

List of Tables

Table 1. Acceleration reading from different function generator inputs. Discrepancies between the two accelerometers was greatest at lower frequencies. As frequency increased, the difference in accelerations were reduced.	54
Table 2. Comparison of ADXL 335 and the handheld accelerometer at 60 Hz. The function generator was set to 60 Hz and a range of voltage potential was set form 1V to 5V. A 1V input showed a 24% difference. 2V and 3V inputs had a difference of 20.5% and 20.3%.....	56
Table 3. Comparison of ADXL 335 and the handheld accelerometer at 126 Hz.	56
Table 4. Comparison of ADXL 335 and the handheld accelerometer at 160 Hz.	57
Table 5. Comparison of FRTL-5 cell metabolic activity after vibration with TRB or voice coil bioreactor.	58
Table 6. Comparison of ROS activity with the TRB and voice coil system.	59

List of Figures

Figure 1. The thyroid is located directly below the larynx in the anterior of the neck (4).	2
Figure 2. Thyroid hormone production (9).....	3
Figure 3. Current method of treatment for different levels of hypothyroidism (34, 35).	8
Figure 4. TSH and forskolin alter actin fiber alignment in thyroid epithelial cells. The top and middle images show that actin fiber align in a flatter orientation when TSH is removed. When TSH or forskolin are returned to the media, thyroid epithelial cells lose some of the actin fiber alignment and tend to ball up (62).....	12
Figure 5. Bioreactor. (A) Image of the TRB enclosed in an environmentally controlled chamber. (B) Schematic of the components of the multi-disc assembly, including the locations of the eight wells used in each study. Four of the wells were chemically stimulated with TSH in addition to receiving oscillatory mechanical signals. The other four wells received no TSH. ..	19
Figure 6. FRTL-6 Metabolic activity and ROS production. (Top). Oscillation significantly increased FRTL-5 cell metabolic activity compared to no oscillation both with and without TSH (* p = 0.0244, ** p = 0.0014, *** p = 0.0002, **** p < 0.0001). (Bottom) Oscillation significantly increased ROS.	24
Figure 7. Gene expression normalized to 18s and to control (i.e., no oscillation, no TSH). (A) The combination of TSH and oscillation (TSH+OSC) resulted in a 100% increase in thyroglobulin expression (p = 0.0406). (B) Sodium iodide symporter (NIS) expression increased approximately 3 to 5-fold (though not significantly) for all three cases of stimulation compared to controls.....	25
Figure 8. cAMP production. cAMP production is increased by TSH and mechanical stimulation. There is a significant increase observed when oscillation and TSH stimulate FRTL-5 cells (p < 0.05).....	26
Figure 9. Metabolic activity of FRTL-5 cells after 5 days of TSH deprivation. Stimulation of FRTL-5 cells after 5 days of TSH deprivation greatly increases the metabolic activity by 24.2% (p < 0.0001).....	32
Figure 10. Metabolic activity after 24 hour TSH stimulation. Metabolic activity increased by 19% after 10 mU/mL of TSH stimulated FRTL-5 cells for 24 hours (* p=0.0022 , n=12).	33

Figure 11. Focal adhesion connection (126).....	36
Figure 12. Metabolic activity increase by oscillation with Y27632 inhibition. Inhibition of the Rho/Rock pathway in FRTL-5 cells did not change their metabolic response to oscillation when compared to previous results. Oscillation of FRTL-5 cells with Y27632 incubation increase metabolic activity by 33.4% (p=0.0012)	41
Figure 13. Oscillation does not increase metabolic activity when actin polymerization is inhibited. Inhibition of actin polymerization affects the FRTL-5 cells ability to sense the oscillation accelerations. There is no significant increase or decrease in metabolic activity. There was a significant increase in metabolic activity for oscillation alone (p < 0.05)	43
Figure 14. Live dead staining of FRTL_5 incubated with cytochalasin D. Live/Dead staining was conducted after vibration of FRTL-5 cells to verify if cells were dying due to vibration and inhibition of actin polymerization (A) with TSH and (B) without TSH.	44
Figure 15. Verification that Y-27632 and cytochalasin D does not inhibit or increase FRTL-5 cells metabolic activity. Y-27632 and cytochalasin D inhibitors do not significantly increase or decrease metabolic activity.	45
Figure 16. Voice coil bioreactor.	49
Figure 17. Labquest 2 data. Acceleration data was collected on the hand held labquest 2 accelerometer. The accelerations were graphed and the peak to peak value was determined for each given input values.....	52
Figure 18. Screenshot of oscilloscope readout. When the oscilloscope is connected to vibrating accelerometer a voltage output waveform is created. The software gives frequency and peak to peak values of the waveform.....	53
Figure 19. Motion created by voice coil.....	60
Figure 20. Metabolic Activity of FRTL-5 cells with a 1-hour vibration/ 1-hour static ratio for 4 hours.	67
Figure 21. Metabolic activity of FRTL-5 cells with a 1-hour static/ 1-hour vibration ratio for 4 hours. Oscillation plus TSH showed the largest increase and significance over the control groups (p < 0.0001). This group also had a significance increase over the TSH activated group (p < 0.05).....	68

Figure 22. Metabolic activity at various accelerations. Accelerations at 4 m/s ² shows a significant increase over control groups (p < 0.05).	69
Figure 23. DNA loss due to oscillation. DNA content of the well decreased slightly from control value for each oscillational accelerations condition. 4 m/s ² showed the largest decrease of 3.314%. There was no significance between any of the groups.	70
Figure 24. ROS at various accelerations. ROS was shown to increase with every conditions. The 6 m/s ² accelerations were also significantly higher than the 2 m/s ²	71
Figure 25. Thyroid follicles (142). (A) Thyroid histology. The round follicle can be seen the center lumen. (B) Polarity of thyroid cell in follicle orientation. (C) Thyroid cell orientation cultured on tissue culture polystyrene.	74
Figure 26. FRTL-5 cells cultured on (A) tissue culture polystyrene (B) collagen type I and (C) basement membrane.	79
Figure 27. Metabolic activity of FRTL-5 cells cultured on adsorbed collagen type I. There was no significance observed.	80
Figure 28. Metabolic activity of FRTL-5 cells cultured on basement membrane. Oscillation and TSH plus oscillation had a significance increase over the control group (p < 0.01).	81
Figure 29. Effects of vibration on FRTL-5 morphology. FRTL-5 cells are culture in 6H media (1 mU/mL TSH) (A). This is the typical morphology normally associated with the culture of FRTL-5 cells. When FRTL-5 cells are deprived of TSH, they have a different morphology (B). FRTL-5 cells were then exposed to oscillation at 1 m/s ² for 24 hours (C). The morphology appears to have shifted back to more rounded shape similar to growth in 6H media. FRTL- 5 cells were also oscillated in 6H media (D). These cells show a similar morphology to group A.	82

Chapter 1: Introduction

Motivation

In this dissertation, I aim to address the role of vibrational forces on thyroid function. The thyroid is a butterfly-shaped gland located just below the larynx on the anterior of the neck (Figure 1). Past research on the thyroid has mainly focused on hormonal factors and other non-mechanic cues. Recently, the growth in space exploration and the need for humans to maintain proper physiological function in space, the role of hypogravity and mechanical forces on human health are being investigated. Thyroid epithelial cells have been shown to increase thyroid stimulating hormone (TSH) sensitivity in response to mechanical stimuli (1). The mechanical stimuli studied were limited, but included, a constant force seven times that of gravity and small vibrational forces that mimic the vibrations felt during a rocket launch (1, 2).

Another motivating factor for investigating the role mechanical forces play in maintaining thyroid function stems from asking the question, "Why is the thyroid located so close to the vocal cords when it could be located anywhere?" Given the thyroids normal location, this dissertation investigated the thyroid response to the mechanical forces caused by vocalization. Vocalization has been shown to cause vibratory accelerations of 2 m/s^2 on the anterior skin of the neck (3).

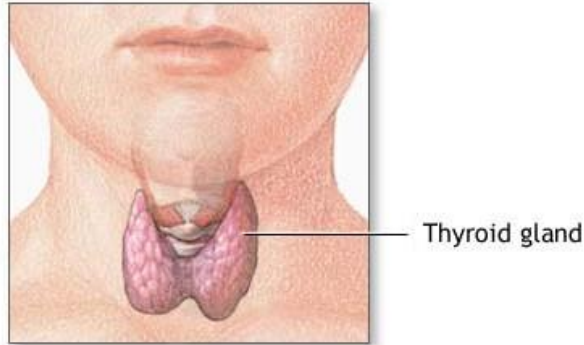


Figure 1. The thyroid is located directly below the larynx in the anterior of the neck (4).

Thyroid Anatomy and Physiology

The process of thyroid hormone production is controlled by thyroid epithelial cells response to thyroid stimulating hormone (thyrotropin, TSH). TSH is a hormone secreted by the pituitary gland in response to low levels of thyroid hormone. TSH can also be signaled for release from the pituitary gland by thyrotropin-releasing hormone, a hormone produced and released by the hypothalamus in response to low levels of thyroid hormone. These hormones are important feedback mechanisms, since TSH is directly responsible for thyroid hormone production in a dose dependent manner (4). TSH activation of thyroid epithelial cells initiates two cascades: the Gs and Gq pathways (5). Activation of the Gs pathway is responsible for the release of hormones and cell proliferation, whereas activation of the Gq pathway increases hydrogen peroxide production and hormone synthesis.

The hormone production process can be seen in Figure 2. Thyroid follicular cells are responsible for iodine uptake and storage (6). Iodine comes mainly from our diets and is transported into thyroid follicular cells by the sodium iodine symporter (NIS) (7). Once iodine is transported into the thyroid, follicular cells iodinate selected tyrosine amino acids of the thyroglobulin protein. For the follicular cells to iodinate the tyrosine amino acid, iodine must first be oxidized. Oxidation of iodine occurs via thyroperoxidase (TPO) and hydrogen peroxide (8). Once the tyrosine amino acids are iodinated, the thyroglobulin proteins are cleaved to form the thyroid hormones thyroxine (T₄) and triiodothyronine (T₃), which are then released into the bloodstream.

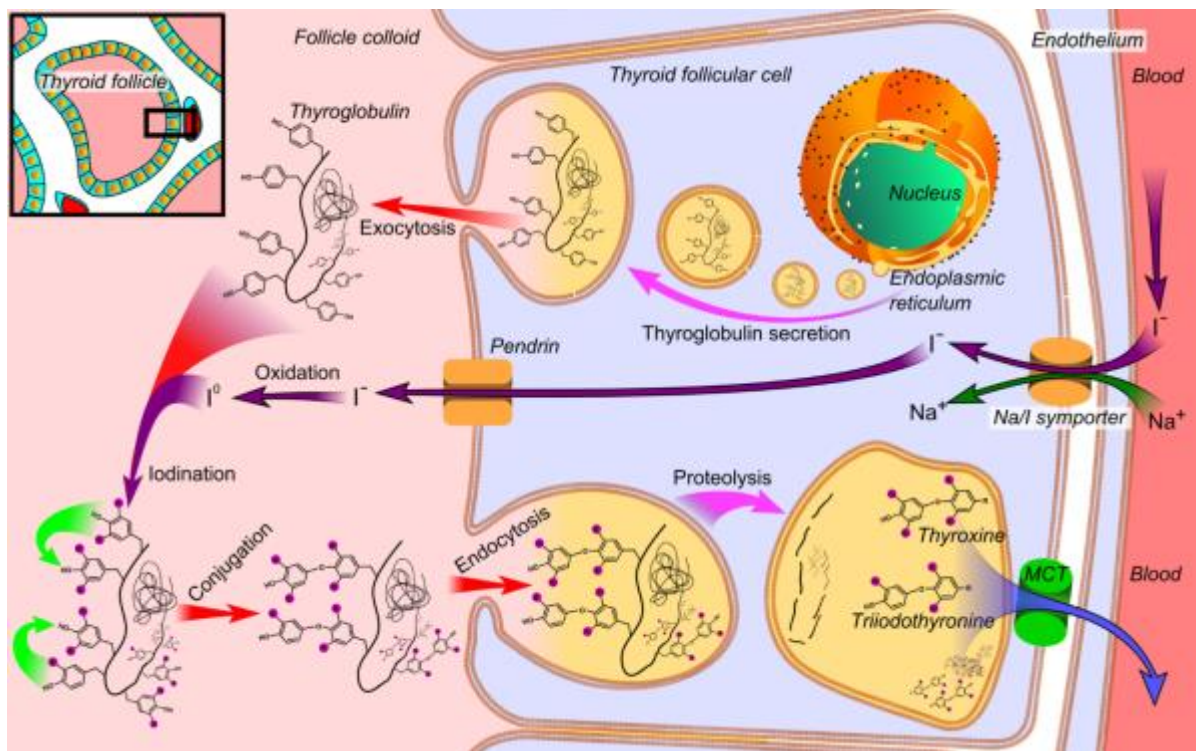


Figure 2. Thyroid hormone production (9).

Current Complication with Thyroid Health

Hypothyroidism, the under production of thyroid hormones, is the most common endocrine disease. It affects around 4% of the population. The two main hormones produced by the thyroid are T₃ and T₄. T₄ being produced in quantities about 4 times greater than T₃. T₃ is more bioavailable than T₄, but T₄ is converted to T₃ for physiological use (10, 11). T₄ also has a longer half-life when circulating in blood and is mainly converted to T₃ in the liver (12). This way the body has a steady supply of thyroid hormone readily available for use.

Thyroid cancer is the most common endocrine cancer, and its incidence rate continues to grow (13). In recent years, reactive oxygen species (ROS) have gained attention for their role in thyroid cancer (8, 14, 15). The main ROS considered is hydrogen peroxide. Hydrogen peroxide is vital for the production of thyroid hormones. However, excessive hydrogen peroxide production is considered hazardous to thyroid tissue as reviewed by Song *et al.* (8). Thyroid epithelial cells do have intracellular defense mechanisms against excessive hydrogen peroxide production such as catalase and GSH reductase and peroxidase (16, 17). However, the thyroid has high rates of somatic mutations and iodine deficient diets lead to higher rates of nodule formation (14, 18). The high rate of somatic mutations have been linked to an increase in ROS generation (14).

Causes of Hypothyroidism

The primary cause of hypothyroidism in developed countries is Hashimoto's thyroiditis. This condition is where your immune system attacks your thyroid and causes thyroid inflammation. Inflammation can then lead to the under production of thyroid hormones. Surgical thyroidectomy, the removal of part or all of your thyroid, also inhibits your ability to make enough or any of your own thyroid hormones. One of the main reasons for thyroidectomy is thyroid cancer. In 2016, there was a reported 64,300 new cases of thyroid cancer (13). Hypothyroidism can also occur from a lack of iodine and is more common in areas where there is not enough iodine in the diet. Another method for the development of hypothyroidism would be a disruption in TPO or hydrogen peroxide production within thyroid epithelial cells (19, 20). A disruption in one of those mechanisms would not allow iodine to be oxidized and result in low levels of thyroid hormone secretion and elevated serum TSH levels. Elevated TSH levels are usually associated with hypothyroidism due to the lack of T₃ and T₄ production. A TSH level above 10 mU/mL is often seen in patients with hypothyroidism.

Subclinical hypothyroidism is another condition of concern. Subclinical hypothyroidism is when a patient has a serum T₄ level within the specified range but a slightly elevated TSH range (typically between 5 mU/L to 10 mU/L). A study in Colorado has shown that 9% of the test subjects had subclinical hypothyroidism (21). It is suggested that patients with subclinical hypothyroidism may be undertreated.

Complications from Hypothyroidism

Symptoms of hypothyroidism include lack of energy, weight gain, dry skin, cold intolerance, and poor memory. Hypothyroidism is more common in females than males (22). Other complications from hypothyroidism include higher rates of osteoporosis and coronary disease in women (23, 24) . Depression has also been shown to increase in subjects with hypothyroidism (25). Whereas most of these symptoms present themselves in patients with hypothyroidism, they don't always appear in patients with subclinical hypothyroidism. Even without any symptoms, it is important to screen for TSH and thyroid levels. It has been shown that patients with subclinical hypothyroidism can still have other complications. These complications includes an increase in serum levels of cholesterol and low-density lipoproteins (26).

Current Treatments

Current treatments for hypothyroidism center around the use of synthetic hormone tablets. The National Health and Nutrition Examination Survey showed that 6.9% of the U.S. adult population surveyed use thyroid hormone replacement (27). Figure 3 shows the standard practice for synthetic drug treatment. This treatment is intended to increase thyroid hormone levels in the body and eliminate the negative symptoms associated with hypothyroidism. However, treatment is not always successful. A study in Colorado showed that 37.2% of the patients receiving thyroid hormone replacement had inadequate thyroid hormone levels (28). Another study reported that 29.6% of the samples had TSH levels above the excepted range (29). Levothyroxine, one of the major synthetic thyroid hormone replacement drugs, also has known complications when

combined with certain drugs and supplements, such as calcium and caffeine (30). Since hypothyroidism patients have to ingest their hormone replacement pills, the timing on when to take thyroid hormone replacement is of concern. This issue can be seen in conflicting studies on when to take levothyroxine (31-33).

The use of desiccated porcine hormone is an alternative treatment method for hypothyroidism. Hormone replacement from desiccated porcine thyroid tissue is sometimes preferred because it contains T₃ and T₄; however, the concentrations of T₃ and T₄ are not the same as produced in human. This treatment may also be better because T₃ and T₄ are produced by thyroid tissue and not in a lab.

Thus, issues concerning the effectiveness of current treatments, the cost of treatments, and concerns over overtreatment necessitates the development of new therapeutic strategies. The method proposed here is the use of mechanical vibrations to stimulate thyroid hormone release. This method might stimulate thyroid hormones naturally and in a more physiological concentration.

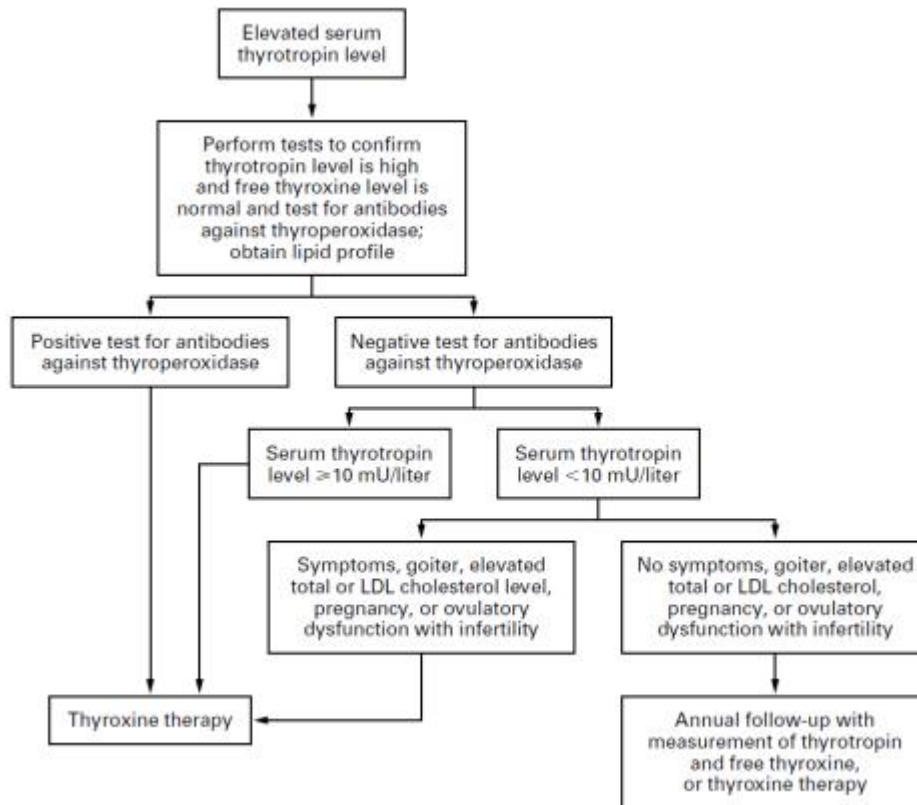


Figure 3. Current method of treatment for different levels of hypothyroidism (34, 35).

Gravitational Forces Acting on the Thyroid

In the last half century, expansion of human exploration into space has accelerated from relatively short trips to the moon to long stays on the international space station. The human body, however, evolved on earth with a constant gravitational force. As such, the lack of gravity in space has led to complications when humans spend an extended time in space. These complications include a loss of muscle mass and bone density (36, 37). More recently, it has been shown that the thyroid is also affected (38). To stimulate thyroid epithelial cells in space, Meli *et al.* conducted experiments with

thyroid epithelial in a clinostat (device to mimic a hypogravity environment) and measured their response to TSH. It was determined that thyroid epithelial cells did not respond to TSH in the clinostat as well as the 1G control (39). This response to TSH has also been shown to increase when thyroid epithelial cells are exposed to a hypergravity environment (1).

These data on how the gravitational environment affects the thyroid tissue has lead me to hypothesize that the thyroid requires mechanical stimulation to function properly, and that mechanical vibrations from vocalization are an important component of that stimulation.

AIM 1: Investigate if vibrational forces help stimulate thyroid hormone.

An alternative to the current treatment methods for hypothyroidism is to stimulate the thyroid hormone production without TSH activation via mechanical stimulation. I propose that vocalization or use of an external device that applies vibrational forces to the thyroid gland for this purpose. Vocalization is one idea because of the thyroid's proximity to the vocal cords (Figure 1), and vocal fold vibration have been shown to cause skin accelerations on the anterior neck in close proximity to the thyroid (3).

In humans, vocalization is mainly considered for communication; however, in other species, vocalization has been studied for other applications. For instance, green treefrogs use calling technique as a mating call. In non-calling males, lower levels of corticosterone and higher levels of androgen have been observed (40). These conditions

made them less aggressive and less likely to mate. The use of vocalization by song birds was reviewed by Ritters (41). Here, vocalization was used in multiple situations from mating calls to territorial defense (42). These behaviors were also correlated with elevated testosterone levels. The mechanism by which hormone levels are increased was not investigated, but a correlation between hormone production and vocalization was found. It is tempting to speculate that the increase in hormone production reported could be because of vocalization.

The vibration created by vocalization in humans has been considered for communication (43), but little has been done to investigate if vibrations from vocalization have other effects on the human body. Vibrations in other area of the human body have been studied (44-47). The majority of research has been into the negative effects of external vibrations acting on the human body, such as from workplace exposure (48). Studies have shown that exposure to these vibration over long periods have been associated with risk factors for back pain, hand arm vibration syndrome (HAVS), and more (48-50). There are numerous studies correlating back pain with excessive exposure to vibrations (51, 52). A review of the literature revealed that an increase in exposure time is directly correlated to the percent of back pain complaints (53).

External sources of vibration have also been shown to have a positive effect on the human body. One method under therapeutic consideration is the use of vibrations as a training method (47). On the hormonal side, studies have looked for increase in testosterone and growth hormones levels with and without whole-body vibration methods (47, 54-56). The study conducted by Di Loreto *et al.* did not show any significant increases in testosterone or growth hormone (55). This is in contrast with the other two

studies. One of those studies showed an increase greater than 300% in growth hormones with individuals that performed squats on a vibrating plate as opposed to static squats. Vibration is also used for relaxation. The main method is “OM” chanting. Kalyani *et al.* have shown “OM” chanting to deactivate certain parts of the brain (57). One hypothesis for this effect is vibration conditions of “OM” chanting may activate the vagus nerve. Vocalization has also been considered for other effects on the brain. It has been hypothesized to have a neurosecretory effect on the brain and may affect endocrine balance (58).

Aim 2: Investigate if cellular cytoskeleton plays an important role in sensing vibratory stimulation

To better understand how the macro-environment (*i.e.* muscle mass, bone density, thyroid health) is changed by vibration, some recent studies in bone have been conducted at the cellular level (59, 60). Here, the focus was to increase the cellular response induced by mechanical stimulation, and identify the mechanisms in which a cell senses these mechanical stimuli. Actin fibers in bone cells have been shown to regulate some of these cellular outputs (61). This is interesting due to the fact that actin fibers have also been shown to change in response to a changing exposure to TSH (62). Figure 4 shows the actin fiber difference when exposed to TSH or forskolin as compared to the control with no added hormones. When TSH is removed from the media, thyroid epithelial cells show a distinct actin network organization. Following the addition of TSH, thyroid epithelial

cells become more rounded and the actin cytoskeletal organization changes.

Consequently, an investigation into the effect of mechanical stimulation on thyroid

behavior should also consider changes cytoskeletal organization.

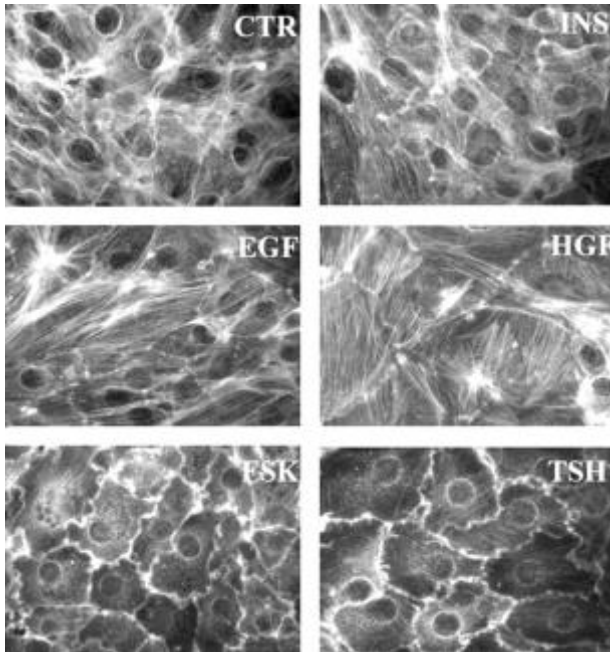


Figure 4. TSH and forskolin alter actin fiber alignment in thyroid epithelial cells.

The top and middle images show that actin fiber align in a flatter orientation when TSH Is removed. When TSH or forskolin are returned to the media, thyroid epithelial cells lose some of the actin fiber alignment and tend to ball up (62).

Aim 3: Investigate if thyroid epithelial cells respond to vibratory stimulation in a dose dependent manner

When studying vibration acting on the human body, three factors of the vibration are taken into consideration: 1) frequency of vibration 2) amplitude of the vibration 3)

duration of vibration exposure. These three factors together are considered the vibration dosage. In the workplace environment, the dosage can be very high. For instance, impact wrench can have an oscillational acceleration around 20 m/s^2 r.m.s. (63). This number only considers the frequency and amplitude. The exposure time can be a full work day for some people. This type of dosage is a lot higher when compared to average whole body vibration training. One whole body vibration study shows the subjects head accelerating around 6 m/s^2 r.m.s with the total vibration exposure not exceeding 3 minutes (44). Experimental design parameters could be changed to increase the dosage. However, one could potentially start to outweigh the positive effects with more serious negative effects.

When studying the effects of vibration on thyroid epithelial cells, we will use an acceleration taken from previous work showing the neck skin accelerations under different vocalization parameters (3). The skin accelerations from this data show acceleration up to 2 m/s^2 . However, the vocal cords are able to produce accelerations much larger than 2 m/s^2 (64). Using this data, I will be able to set a lower limit for the acceleration forces. From there I will be able to increase the acceleration dosage. I will also be able to determine if cycling between vibrating and stationary conditions have an effect.

This dissertation work aims to verify if vibrational forces, similar to what would occur during vocalization, have an effect on thyroid epithelial cells. I also investigated the mechanism in which these cells sense there surrounding mechanical environment. Also, I have investigated if this cellular response is dependent on vibration dosage.

Chapter 2: Test of Aim 1: Vibrational Forces Help Stimulate Thyroid Hormones

The work described in this chapter has previously been published in the following journal. “A.P. Wagner SC, I.R. Titze, E.A. Sander. Vibratory stimulation enhances thyroid epithelial cell function. *Biochemistry and Biophysics Reports*. 2016;8:376-81.”

Introduction

The tissues of the body are routinely subjected to various forms of mechanical vibration, the frequency, amplitude, and duration of which can contribute both positively and negatively to human health (46). Small doses of vibration may promote tissue growth (65), whereas large doses can result in tissue damage (66). An example of the later is hand-arm vibration syndrome (HAVS), where the operation of vibrating power tools can produce chronic and progressive dysfunction to the vascular, muscular, and neurological systems (50, 67). Several studies on HAVS have demonstrated a connection between mechanical vibrations and an adverse cellular response, such as vascular complications in response to increased reactive oxygen species (ROS) production (68-70). In contrast, whole body vibrations have been positively associated with substantial increases in hormone production (47, 55, 71), possibly through direct mechanical stimulation or enhanced biomolecular transport.

These studies suggest that mechanical vibrations could play an important role in regulating hormone production and ROS in the endocrine system. The most common

endocrine disease, hypothyroidism, affects approximately 5% of the population (72). It is characterized by a decrease in thyroid hormone production that stems in part from a reduction in thyroid epithelial cell sensitivity to thyroid stimulating hormone (TSH). In order for these hormones to be produced, iodine must be transported into the thyroid epithelial cells through the sodium iodine symporter (NIS). Iodine must then be oxidized by thyroid peroxidase (TPO) and the ROS hydrogen peroxide (H_2O_2) and added to the tyrosine residues of thyroglobulin (TG). The iodized tyrosine residues are then cleaved to form the thyroid hormones triiodothyronine (T_3) and thyroxine (T_4), which are critical for regulating cell metabolism, growth, and development (73).

There is evidence that mechanical stimulation can positively influence TSH sensitivity. Several *in vitro* studies have demonstrated that thyroid epithelial cells are responsive to their mechanical environment, particularly in the context of altered gravity and space exploration (1, 74). For example, Meli *et al.* found that Fischer rat thyroid line-5 (FRTL-5) cells had decreased sensitivity to thyroid stimulating hormone (TSH) after exposure to a hypogravity situation (74). In contrast, FRTL-5 exposure to a 7g centrifugal force increased TSH receptor (TSHR) number and responsiveness to TSH (1). The difference in outcomes could be in part due to an increase in reactive oxygen species (ROS) production in response to an altered mechanical environment, particularly as ROS are vital to thyroid hormone production. Too much ROS, however, can be detrimental to thyroid health (14, 15), with excess ROS implicated as the basis for the high rate of cancer found in the thyroid (75).

The vocal cords, which are typically in close proximity to the thyroid, may also supply the thyroid with important mechanical signals that modulate hormone and ROS production via mechanical vibrations from phonation. In order to explore the possibility that vibrational stimulation from vocalization can enhance thyroid epithelial cell function, we subjected FRTL-5 cells to physiological vibrations in a well-characterized, torsional rheometer-bioreactor (76-78) and compared their response to TSH stimulated cells.

Materials and Methods

Cell Culture

Fischer rat thyroid line cells (FRTL-5, American Type Culture Collection, Rockville, MD, CRL 8305) derived from the normal thyroid gland of Fischer rats were maintained in a 37 °C humidified incubator supplied with 95%/5% air/CO₂. FRTL-5 cells were cultured according to the supplier's recommendations in Ham's F12K medium with 2 mM L-glutamine and adjusted to contain 1.5 g/L sodium bicarbonate. 0.5% bovine calf serum and six additional hormones required for FRTL-5 cells to proliferate and maintain thyroid function were added to the medium, as specified by the originators of this cell line (79, 80). These six hormones included 1 mU/ml thyroid stimulating hormone (TSH), 0.01 mg/ml insulin, 10 nM hydrocortisone, 0.005 mg/ml transferrin, 10 ng/ml somatostatin, and 10 ng/ml glycyl-L-histidyl-L-lysine acetate (All reagents from Sigma, St Louis, MO) (81). Growth medium was used for cell expansion and to acclimate the cells prior to initiating the experiments. For the experiments, growth medium was modified so that it either contained 10 mU/ml TSH or no TSH as indicated below. Cells

were passaged at 70% confluency and harvested at passages four through eight for the experiments.

Application of Physiological Vibrations with a Torsional Rheometer-Bioreactor

With the Torsional Rheometer-Bioreactor (TRB) previously developed in our lab (76), physiological forces can be applied to adherent cells in a multi-well disc by specifying the frequency, amplitude, and duration of vibration (Fig. 1). Briefly, 96 well tissue-culture plates were cut into 57 mm diameter, multi-well discs so that the plates could be positioned in the TRB. The plates, which were previously sterilized by the manufacturer, were covered with a sterile adhesive to prevent debris from entering the wells during cutting with a jigsaw and to preserve sterility. Next, trypsin/EDTA (Life Technologies, Grand Island, NY) was used to release FRTL-5 cells from the tissue culture flasks. The cells were centrifuged at 1500 rpm for 5 minutes, re-suspended in complete media, and then plated at a density of 10,000 cells/well to each of the eight outer wells of the disc, each of equal radial distance from the disc center. FRTL-5 cells were also re-plated at the same density in wells of a 96-well plate to serve as controls (n=8). Cellular attachment was allowed to occur in all wells for 48 hours in growth medium (i.e., with 1 mU/ml TSH) before TSH was completely removed from the growth medium for an additional 48 hours of culture. TSH deprivation between 1 and 10 days is frequently employed (*e.g.*, (82, 83)) prior to beginning an experiment because it greatly increases FRTL-5 sensitivity to the reintroduction of TSH (79), and because deprivation is thought to control cell synchronization (84). We chose a deprivation period of 48 hours followed by re-exposure to 10 mU/mL TSH based on other studies that used similar

parameters (85, 86). In particular, we used the study by Bjorkman *et al.* (85) as a guide, where they showed a significant increase in hydrogen peroxide production with two days of TSH deprivation followed by 10 mU/mL of TSH. Immediately following this 48 hour TSH-free culture period, 10 mU/mL of TSH was added back to growth medium supplied to half of the wells in the multi-well disc (n=4) and to half of the wells in the control plate (n=4). The other half of the wells received growth medium without any TSH. The multi-well discs were then mounted onto the TRB and subjected to four conditions: (1) no oscillation and no TSH; (2) no oscillation and TSH; (3) oscillation and no TSH, (4) oscillation and TSH. The oscillatory conditions for this study were selected based on vibrational parameters related to vocalization (87). The TRB was set up to apply inertial forces to the adherent cells in the form of oscillatory accelerations of 2 m/s^2 , based on accelerations measured on the skin in front of the thyroid (88). In addition, the experiments were conducted at a torsional frequency of 126 Hz, a frequency within the range of a typical adult male voice and corresponding to the characteristics of American speech and the daily voice usage of public school teachers (87). Finally, the stimulation was applied constantly (*i.e.*, a duty ratio of 1) for the full duration of the experiment (*i.e.*, four hours) in order to produce for this pilot study what we hypothesized would be a maximum effect from mechanical stimulation. Four hours was selected in order to be consistent with prior experiments conducted with vocal fold fibroblasts (76) and because t-tests from a preliminary study indicated significant differences in metabolic activity ($p = 0.0154$) between TSH deprived and TSH stimulated groups after only four hours.

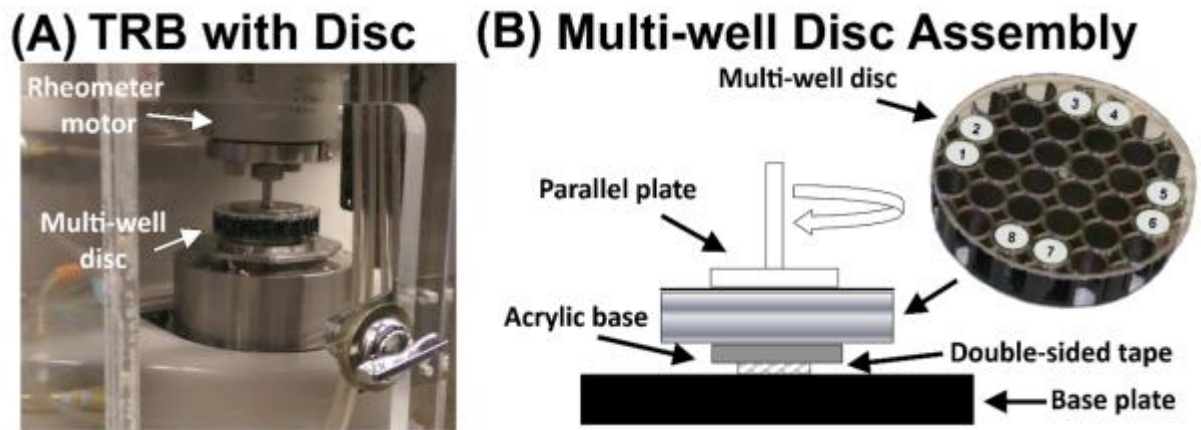


Figure 5. Bioreactor. (A) Image of the TRB enclosed in an environmentally controlled chamber. (B) Schematic of the components of the multi-disc assembly, including the locations of the eight wells used in each study. Four of the wells were chemically stimulated with TSH in addition to receiving oscillatory mechanical signals. The other four wells received no TSH.

Quantification of Metabolic Activity

Alamar Blue (AlamarBlue®, Life Technologies, Grand Island, NY) was used to quantify differences in metabolic activity in response to exposure to TSH and oscillatory accelerations (89). A 10x stock solution of Alamar Blue was diluted in calcium and magnesium free PBS to achieve a 1x final concentration. At the conclusion of each experiment, medium was removed, the wells were washed gently with PBS, and 100 μ L of Alamar Blue solution was added to each well. Both the multi-well discs and controls were returned to the incubator for 1 hour. The Alamar Blue solution was then transferred to a black 96-well plate and the fluorescence was measured (Ex/Em = 560/590 nm) with

a fluorometer (FLOUstar, BMG LABTECH Ltd., Ortenberg, Germany). Results are reported in arbitrary fluorescence units (AFU) with the blank value subtracted.

Quantification of Cell Number

Hoechst 33342 (H1399, Life Technologies, Grand Island, NY) was used to quantify cell number. After removal of Alamar Blue, the wells were washed with PBS and 100 μ L of 5 μ g/mL Hoechst in PBS was added to each well, followed by a 30 minutes incubation at 37 $^{\circ}$ C. Fluorescence was measured with a fluorometer (Ex/Em = 380/460 nm) and reported as AFU.

Quantification of Reactive Oxygen Species (ROS) Levels

A dichlorofluorescein (DCF) assay (D399, ThermoFisher) was conducted on a separate set of experiments that were subjected to identical experimental conditions as those for the previous assay in order to measure differences in ROS production (90). After stimulation, media was removed from the wells and replaced with 50 μ L of 10 μ M DCF in PBS solution and incubated at 37 $^{\circ}$ C for 30 minutes. ROS production was measured with a fluorometer (Ex/Em = 495/520 nm) and reported as AFU.

Quantification of Cyclic Adenosine Monophosphate (cAMP) Levels

A direct cAMP assay kit (Enzo Life Sciences, Farmingdale, NY) was used to measure intracellular cAMP concentration (also on a separate set of experiments under

identical experimental conditions) because TSH stimulates thyroid cells primarily through the cAMP signaling cascade (91). Three independent experiments were conducted for each condition. However, due to the low cell densities in this experiment, all four wells for a given experiment and condition were pooled together for one measurement, thus giving a sample size of $n = 3$ for each condition. At the conclusion of each experiment, the FRTL-5 cells were lysed with 100 μL 0.1 M HCl for 10 minutes, centrifuged at 5000 rpm for 5 minutes, and then frozen so that all experiments could be analyzed simultaneously. Following the manufacturer's protocol, an acetylation step was used to increase sensitivity. A 1:2 mix of acetic anhydride:trimethylamine was added at a 5% concentration to the samples and the standards, which ranged from 0.078 pmol/mL to 20 pmol/mL. Neutralizing solution (50 μL) was added to each well of the 96-well cAMP ELISA plate. An additional 100 μL of sample or standard was then added to each well, followed by 50 μL of blue conjugate and 50 μL of yellow antibody. The wells were mixed at 280 rpm for 2 hours. The solution was then removed and the wells were washed 3 times. 200 μL of substrate solution was added to each well and incubated at room temperature for 1 hour. 50 μL of stop solution was then added and the absorbance was measured at 405 nm with a Spectramax i3x (Molecular Devices, Sunnyvale, CA).

Thyroglobulin (TG) and Sodium/Iodine Symporter (NIS) Gene Expression

Assessed with qPCR

TG and NIS gene expression was quantified using qPCR. TG is a precursor protein for thyroid hormone production, and NIS is important for trafficking of iodine into thyroid epithelial cells. Immediately following the stimulation period, FRTL-5 cells

were removed from the multi-disc and control plates with trypsin/EDTA. Cells were then centrifuged and wash with PBS before being stored at -20 °C for later analysis. Upon thawing, total RNA was isolated using an RNeasy Mini Kit (Qiagen, Austin, TX, USA) according to the manufacturer's directions. A total of 100 ng of RNA was converted to cDNA via RT-PCR by using a high capacity cDNA reverse transcription kit (Applied Biosystems, MA, USA). The RT-PCR protocol was 10 minutes at 25 °C followed by 37 °C for 2 hours. The resultant cDNA was diluted 1:5 in RNAase free water, then 4.5 µL of the diluted cDNA was mixed with 5.5 µL of TG (Rn00578496_m1) or NIS (Rn00583900_m1) TaqMan miRNA primer and probe mix (1:10 of NIS, TG primer:TaqMan probe solution) (Life Technologies, MA, USA). These reactions were carried out in triplicate. Gene expression levels were measured with an Applied Biosystems 7300 Real Time PCR System (Applied Biosystems, MA, USA) in a 96 well plate with thermal cycling parameters set at 50 °C for 2 minutes, 95 °C for 10 minutes, 40 cycles of 95 °C for 15 seconds, and 60 °C for 1 minute. Steady-state mRNA levels were normalized to 18s rRNA and calculated relative to untreated controls by the relative quantitation using comparative C_T. Because RNA yields were low, all four wells for a given condition were pooled together for one measurement run in triplicate. Three independent experiments were conducted for each condition (i.e., n=3).

Statistical Analysis

All data are presented as mean values \pm standard deviation. Except for the gene expression data and the cAMP ELISA (sample sizes detailed above), these values represent 4 independent experiments, each containing four samples per group (n=16).

The oscillation and TSH condition for the alamar blue and Hoechst assays represents $n = 15$ samples because one sample was discarded due to a sample processing error.

Anderson-Darling tests were conducted first to confirm that the data were not from non-normal distributions. One-way analysis of variance (ANOVA) with post hoc Tukey tests (Prism 7, GraphPad) were then used to determine statistical significance.

Results

Changes in FRTL-5 cell metabolic activity were affected in a stimulation dependent manner (Fig. 6A). The addition of TSH increased metabolic activity 11% (though not significantly, $p = 0.107$) compared to the unstimulated control (i.e., no TSH and no oscillation). Oscillation alone also had a significant effect on metabolism ($p = 0.0014$), increasing it by 20% compared to control. The combination of oscillation and TSH significantly increased metabolic activity further (33%) compared to control ($p < 0.001$). Relative levels of ROS produced in response to TSH and oscillatory stimulation mirrored the trends observed for metabolic activity (Fig. 6B). TSH alone increased ROS production 10% compared to controls. Oscillation alone and oscillation with TSH increased significantly ROS production 24% ($p = 0.0077$) and 36% ($p < 0.0001$) compared to controls, respectively. For all testing conditions, the FRTL-5 cells grew into clustered multicellular aggregates over the course of the experiment. No significant differences in cell number were observed amongst the conditions tested (Fig. 6C), indicating that mechanical and chemical treatments did not affect cell attachment to the substrate.

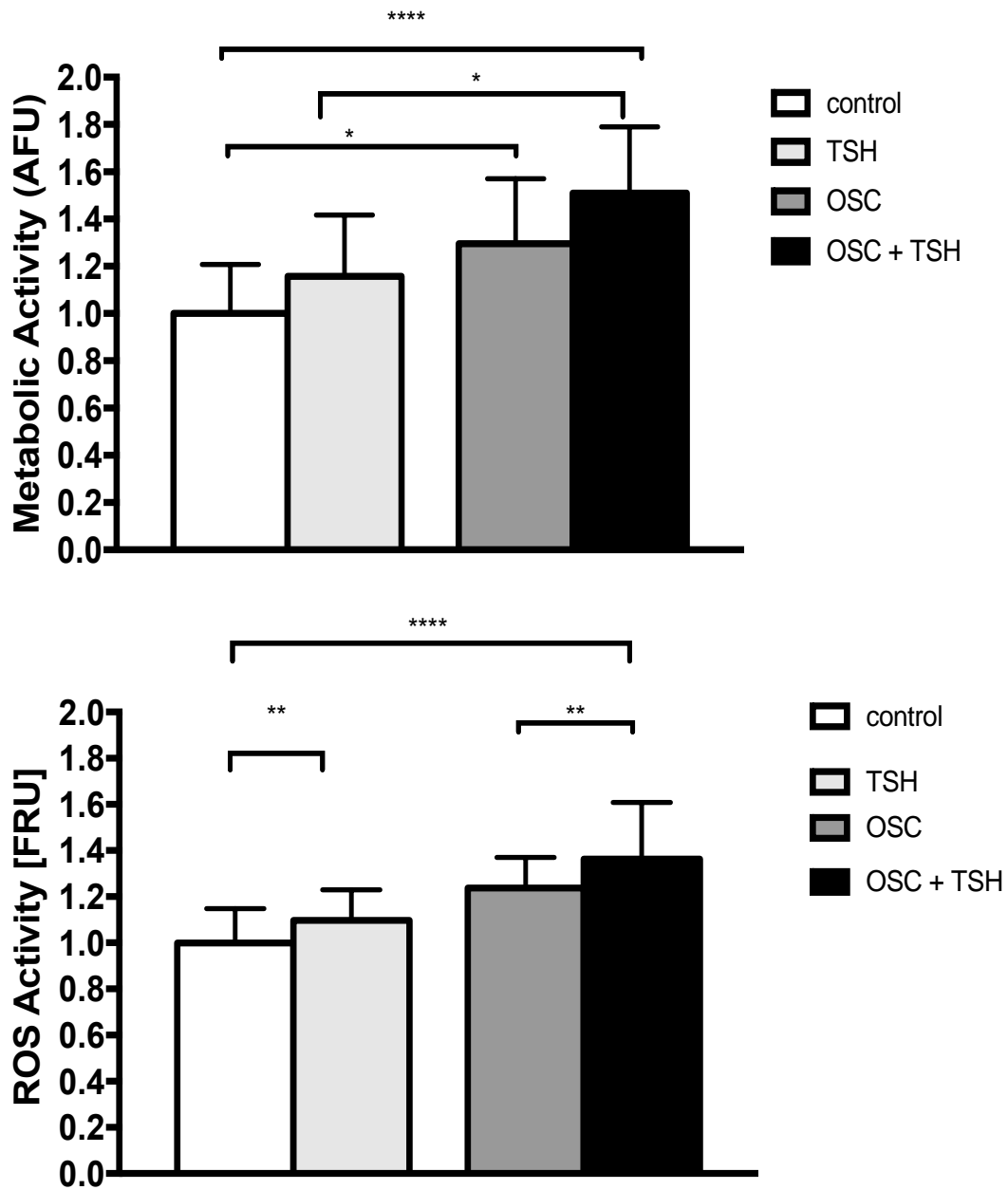


Figure 6. FRTL-6 metabolic activity and ROS production. (Top). Oscillation significantly increased FRTL-5 cell metabolic activity compared to no oscillation both

with and without TSH (* $p = 0.0244$, ** $p = 0.0014$, *** $p = 0.0002$, **** $p < 0.0001$).
(Bottom) Oscillation significantly increased ROS.

Gene expression was also dependent on the stimulation conditions. Relative TG gene expression remained unchanged in response to TSH alone (Fig. 7A). TG expression increased 25% with oscillation alone and nearly tripled ($p = 0.0406$) with the combination of oscillation and TSH compared to control. NIS expression (Fig. 7B) was highly variable and increased approximately three to five-fold in response to all forms of treatment compared to control.

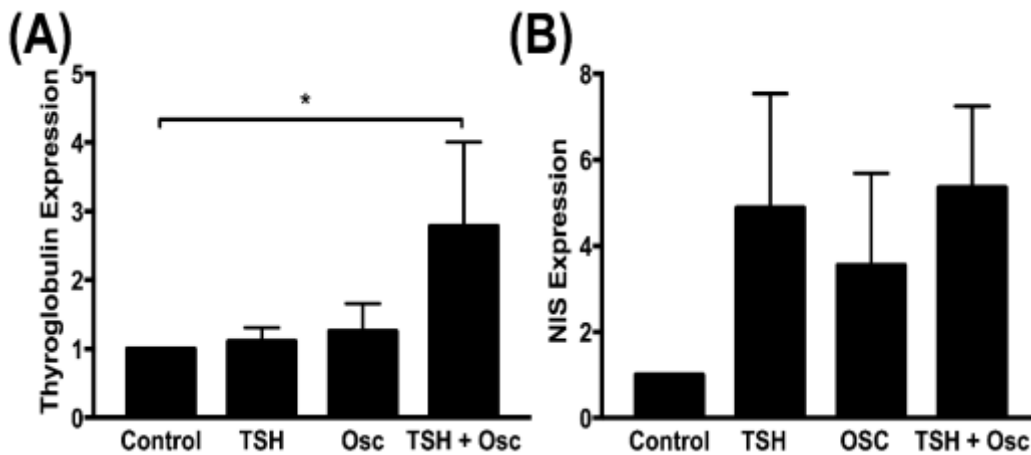


Figure 7. Gene expression normalized to 18s and to control (i.e., no oscillation, no TSH). (A) The combination of TSH and oscillation (TSH+OSC) resulted in a 100% increase in thyroglobulin expression ($p = 0.0406$). (B) Sodium iodide symporter (NIS) expression increased approximately 3 to 5-fold (though not significantly) for all three cases of stimulation compared to controls.

Because TSH acts primarily through the cAMP signaling cascade (91), cAMP levels for each condition were also measured in order to determine if oscillation also triggers an increase in cAMP (Fig. 8). The baseline cAMP concentration measured in the unstimulated control group was 0.816 ± 0.344 pmol/mL. The concentration increased 2.3 fold in response to oscillation alone (1.866 ± 0.853 pmol/mL) and 3.5 fold in response to TSH alone (2.870 ± 0.894 pmol/mL) compared to controls. Together, the combination of TSH and oscillation significantly ($p = 0.0121$) increased cAMP levels 5.5 fold at 4.452 ± 1.663 pmol/mL compared to controls.

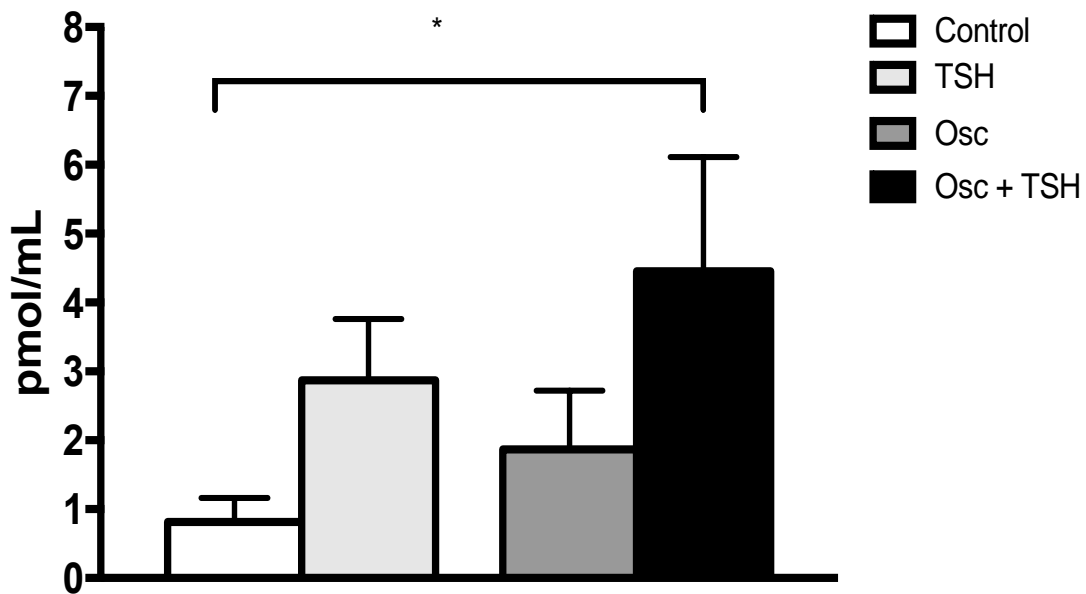


Figure 8. cAMP production. cAMP production is increased by TSH and mechanical stimulation. There is a significant increase observed when oscillation and TSH stimulate FRTL-5 cells ($p < 0.05$).

Discussion

Given that mechanical vibrations have been associated with a positive increase in hormone production (47, 55, 71), and that the thyroid is in close proximity to the vocal cords, we hypothesized that thyroid hormone production could also be positively stimulated by the vibrational forces of phonation. In order to begin to test this hypothesis, we subjected adherent FRTL-5 cells to oscillatory inertial forces from rotational oscillatory motion that approximates the accelerations thyroid cells might experience during typical phonation.

We then measured changes in metabolism, ROS production, and TG and NIS gene production as indicators of enhanced thyroid function because each of these components is vital to thyroid hormone production, and because each has been shown to increase in response to hormonal stimulation with TSH (85, 92, 93). We reasoned that if inertial forces from oscillation are capable of providing the same (or similar) stimulatory effects as TSH, one should expect to see comparable increases to those from TSH stimulation alone. The FRTL-5 cells responded to mechanical stimulation with increased metabolic activity, increased ROS production, and increased gene expression of NIS and TG compared to un-stimulated controls, and showed an equivalent or greater response than TSH only stimulated cells. Taken together, these results suggest that mechanical vibrations could provide stimulatory cues that help maintain thyroid function.

Which signaling pathways are activated by these mechanical cues is unclear. TSH stimulates rat and human thyroid cells primarily via an increase in intracellular cAMP, which in turn activates several additional signaling pathways (91). In order to determine if mechanical stimulation also operates through the same cAMP signaling cascade as

TSH does, we measured intracellular cAMP levels and found that they too increased with oscillation. The cAMP trends did, however, differ some from the trends for metabolic activity and ROS. Specifically, cAMP was lower when only oscillations were applied than when only TSH was administered. Although not significantly different from each other, this trend was flipped with respect to the trends found for metabolic activity and ROS.

It is possible that a difference in cAMP levels between the oscillation and TSH groups exists, and that this difference would become significant with a larger samples size. If this is the case, this difference might indicate that other signaling mechanisms are also operating that could be differentially regulated depending on whether the stimulus is mechanical, hormonal, or a combination of the two. Such mechanisms could operate parallel to the cAMP cascade, such as the phosphoinositide phospholipase C (PLC) pathway (91, 94), or they could interact further downstream of cAMP, such as MAPK (91, 95). For example, modulation of the MAPK/EK pathway through mechanical stimulation has been demonstrated in other cell types (96), and could play some role here. Further investigation will be required to determine precisely which pathways are activated by vibrational stimulation.

The positive effects of vibrational stimulation have been noted by others, particularly as a potential therapy for fostering an anabolic response in the musculoskeletal system (97, 98). Of particular relevance to this study are the reports on high frequency, low-amplitude mechanical signals (LMS) and their role in regulating osteogenesis, musculogenesis, and other adaptive cellular responses (61, 99-105). LMS is characterized by strains so low as to be considered negligible (i.e. peak strains are on the

order of 1-2 microstrain) (99)). In our experiments, the FRTL-5 cells were attached to stiff tissue culture polystyrene (TCP), which we assumed also experienced negligible deformations during oscillation. Without a deformable substrate, gene transcription cannot ostensibly be triggered by the well-characterized outside-in signaling pathway in which mechanical cues are transmitted from the ECM to the cytoskeleton via transmembrane focal adhesions and on to the nucleus (99). The underlying mechanisms responsible for an adaptive cellular response to LMS remain unclear. Recently, Uzer *et al.* found that the LINC (linker of nucleoskeleton and cytoskeleton) complex, a collection of proteins that mechanically couples the cytoskeleton to the nucleus, appears to play an important role in the cellular response to high frequency, LMS (61). They observed that LMS applied to mesenchymal stem cells facilitated focal adhesion kinase (FAK) and Akt phosphorylation, actin cytoskeletal reorganization, and force transmission to the nucleus via the LINC complex (61). When the LINC complex was disabled these adaptive responses to LMS disappeared. Others have also provided evidence that LINC helps maintain a balance of forces between the nucleus and the actin cytoskeleton, and that dynamic changes in the homeostatic state of stress in the cytoskeleton can transfer localized deformations/forces to the nucleus, which in turn mechanoregulates gene transcription and other cellular activities (106-109). In the context of LMS, it appears feasible that force generation can originate internally from the mechanical deformations created by the passive response of the denser nucleus (60, 61) due to acceleration from the oscillatory rotational motion imposed on the multi-well disc by the TRB.

Another possible source of mechanical stimulation is from fluid shear stress. In our system, each well was filled completely with culture medium in order to reduce shear

stresses caused by sloshing of the culture medium. Smooth particle hydrodynamic computational simulations predicted that shear stresses decrease with increasing fluid height in the well, and that for similar TRB operating conditions the peak shear stresses should be less than 0.01 Pa (110). Although these shear stresses are quite small in the TRB, it is still possible that they also are a source of mechanical stimulation *in vivo* when movement is less confined. For example, similar to our study, computational simulations on the effect of LMS on osteocytes *in vitro* conclude that membrane deformations from fluid shear stresses are too low to be stimulatory (111). However, simulations of LMS on trabecular bone *in vivo* estimate median shear stresses between 0.3 and 1.1 Pa that are considered high enough to produce an anabolic effect (112). Clearly more investigation is required to determine which mechanical mechanisms might be responsible for LMS's effect on cell behavior.

In this initial study, We chose to apply a vibration frequency, acceleration, and duration that was comparable to our previous work with vocal fold fibroblasts for an adult male voice with a teacher-student contact time of 4 – 6 hours (76). However, the parameter space mimicking human phonation is quite large. As such, it should be noted that the current study does not indicate if higher or lower frequencies, accelerations, duty cycles, or durations, as may occur in other settings (e.g., musicians and high vocal professionals), causes more or less metabolic activity, ROS production, and TG/NIS gene expression, or whether such activities are beneficial or harmful to thyroid and overall health.

The culture condition parameter space for FRTL-5 cells is also quite large. Although FRTL-5 cells are a well-characterized cell line for studying thyroid function,

culture conditions, including the length of TSH deprivation, the concentration of TSH during re-exposure, and the duration of re-exposure for the experiment, vary widely (91, 113). Data from our lab do show an even greater increase in metabolic activity when FRTL-5 cells are deprived of TSH for 5 days (Figure 9). For this pilot study, our culture conditions were within the ranges reported in the literature (e.g., (85)). However, the four hour TSH re-exposure time we chose was shorter than the 24-48 hours most commonly employed (though not outside the range of reported values). We picked four hours in order to be consistent with prior experiments conducted in our lab with vocal fold fibroblasts (76) and because t-tests revealed a statistically significant 11% increase in metabolic activity ($p = 0.0154$) in TSH stimulated groups compared to no TSH after four hours. However, when we repeated the experiment with the two additional oscillation groups, a one-way ANOVA indicated that the positive control was no longer significantly different from the negative control because the variance now associated with four groups had increased. In a follow up experiment, we measured metabolic activity after 24 hours of stimulation with TSH (positive control) versus no TSH (negative control) and found that metabolic activity increased 19% compared to 24 hours with no TSH (Figure 10, $p < 0.0022$), indicating that longer re-exposure times should significantly increase the response of the positive controls.

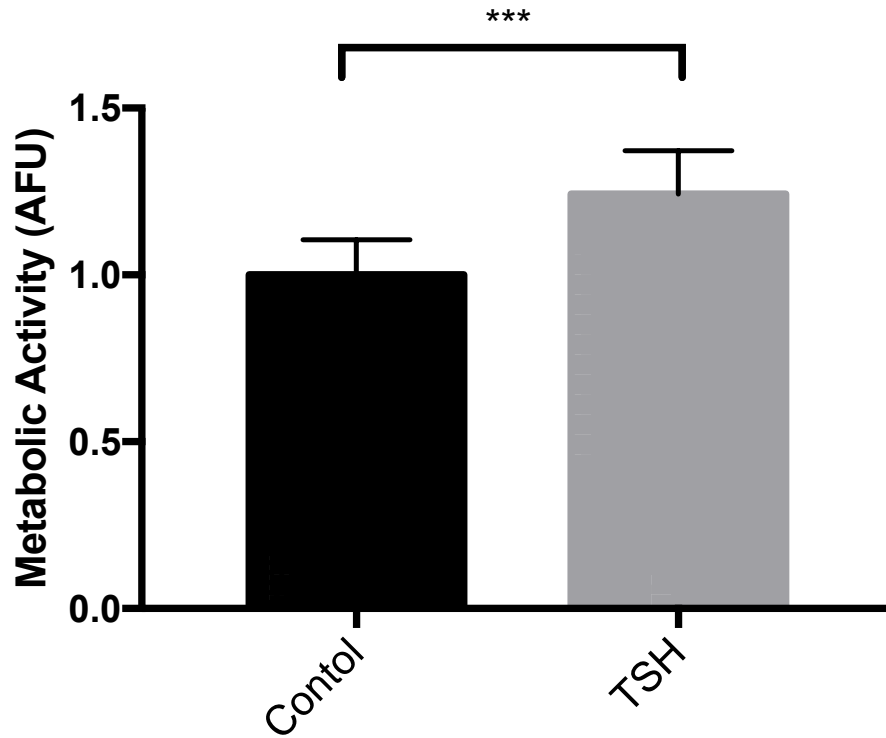


Figure 9. Metabolic activity of FRTL-5 cells after 5 days of TSH deprivation.

Stimulation of FRTL-5 cells after 5 days of TSH deprivation greatly increases the metabolic activity by 24.2% ($p < 0.0001$).

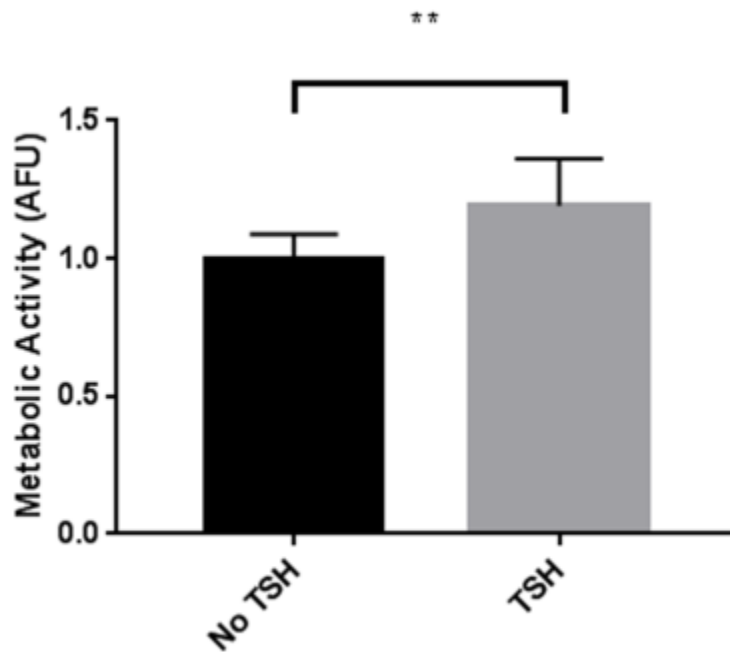


Figure 10. Metabolic activity after 24 hour TSH stimulation. Metabolic activity increased by 19% after 10 mU/mL of TSH stimulated FRTL-5 cells for 24 hours (* p=0.0022 , n=12).

In addition to exploring the vibrational and culture condition parameter space further, future investigations on the effects of vibratory stimulation of FRTL-5 cells will also require the development of a more physiological culture system that better reflects the *in vivo* structure and physiology of the follicle (114). Although FRTL-5 cells are well characterized, and they replicate many of the functions of the thyroid, including TSH sensitivity and thyroglobulin production/secretion (74), the cells used in this study were maintained in monolayer on hard TCP, the stiffness of which greatly exceeds that of the ECM of soft tissues. Several recent studies have demonstrated that many cell activities,

including differentiation, can be regulated by mechanical cues such as substrate stiffness (115-117) and dimensionality (2D vs. 3D) (118). In fact, thyroid epithelial cells cultured in static 3D collagen gels do form follicles with structural polarity (114, 119, 120), presumably because of favorable mechanical and compositional cues. Our next steps will be to translate our findings here to a similar 3D collagen gel system (121).

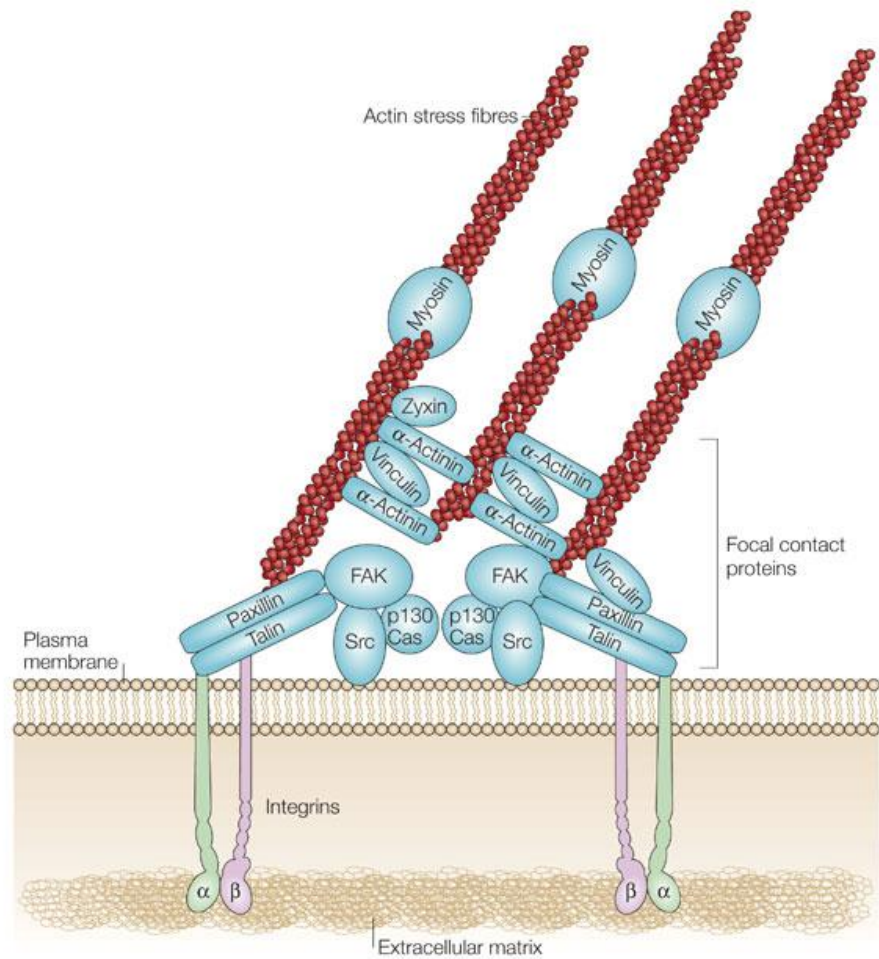
In conclusion, these pilot data are supportive of the possibility of using vibrations from phonation to stimulate thyroid hormone production and for augmenting existing treatments for some thyroid-related diseases. A phonation-based treatment could also be beneficial for offsetting the negative effects of microgravity on the thyroid, a situation of particular importance to those subjected to extended space travel.

Chapter 3: Evaluate Aim 2: Cellular Cytoskeleton Plays an Important Role in Sensing Mechanical Forces

Introduction

The human body is constantly exposed to a number of mechanical forces that are transmitted down to the cellular level. One area where this is most notable is in bone cells. Much work has focused on applying a shear stress from fluid flow or strain from substrate deformations (122, 123). Both of these systems apply forces that alter the cell's cytoskeleton. The TRB applies oscillational forces to a multi-well disc and these forces are directly translated to adherent cells. A similar approach to vibrational forces induced by the TRB were presented by Rosenberg *et al.* (124). In this study, a frequency range from 20 to 60 Hz and an acceleration less than 0.2G increased proliferation and metabolic activity in bone cells (124). Currently, there are two studies that looked at mechanical forces via vibrations acting on thyroid cells (2, 125). However, these studies on bone and thyroid cells only consider the mechanical input and cellular output.

To understand how cells respond to their surrounds, it is also important to understand how they are connected to extracellular material. Integrins are transmembrane proteins that connect cells to extracellular matrix proteins (ECM). They are comprised of an α and β subunit. These subunits are located extracellularly. In the cytoplasm, integrins connect to focal adhesion sites that connect the extracellular integrin to the intracellular actin cytoskeleton structure (Figure 11). This connection plays an important role in cells ability to sense and respond to external forces (61).



Nature Reviews | Molecular Cell Biology

Figure 11. Focal adhesion connection (126).

Focal adhesions have been linked with many of mechanical stimuli previously mentioned. It has been shown that pulling a material to stretch a cell increase the cells focal adhesion size (127). Cells located in the heart have also shown cellular function changes due to a change in their mechanical surrounds. Focal adhesions have a direct impact on the cells ability to sense these mechanical stimuli (128, 129).

In addition to focal adhesion, the Rho/Rock pathway has also been investigated for its role in mechanosensing.. It has been shown that when Rho/Rock is blocked they lose their ability to adjust to ECM stiffness (130, 131). Mechanical cues also affect the cytoskeleton. For example, by causing adjustments in actin organization. Skin fibroblasts under tension increase actin polymerization at focal adhesions (132). Changes in actin polymerization can affect many cell processes, such as mobility and protein trafficking (133, 134). Osteoblasts also lost their ability to sense mechanic stimuli when actin polymerization was disrupted (61). These studies highlight the importance of actin the actin cytoskeleton for mechanosensing. The purpose of this work is to determine if disruption of the actin cytoskeleton and the Rho/ROCK pathway also interfere with the ability of thyroid epithelial cells to sense their mechanical environment.

Materials and Methods

Cell Culture

Fischer rat thyroid line cells (FRTL-5, American Type Culture Collection, Rockville, MD, CRL 8305) derived from the normal thyroid gland of Fischer rats were maintained in a 37 °C humidified incubator supplied with 95%/5% air/CO₂. FRTL-5 cells were cultured according to the supplier's recommendations in Ham's F12 Coon's adjusted to contain 1.5 g/L sodium bicarbonate and 0.5% bovine calf serum. Six additional hormones required for FRTL-5 cells to proliferate and maintain thyroid function were added to the medium, as specified by the originators of this cell line (79, 80). These six hormones included 1 mU/ml thyroid stimulating hormone (TSH), 0.01 mg/ml insulin, 10 nM hydrocortisone, 0.005 mg/ml transferrin, 10 ng/ml somatostatin,

and 10 ng/ml glycyl-L-histidyl-L-lysine acetate (All reagents from Sigma, St Louis, MO) (81). Growth medium was used for cell expansion and to acclimate the cells prior to initiating the experiments. For the experiments, growth medium was modified so that it either contained 10 mU/ml TSH or no TSH as indicated below. Cells were passaged at 70% confluency and harvested at passages four through eight for the experiments.

TRB Setup

The TRB was used to assess the FRTL-5 cells response to oscillations. Trypsin/EDTA (Life Technologies, Grand Island, NY) was used to release FRTL-5 cells from the tissue culture flasks. The cells were centrifuged at 1500 rpm for 5 minutes, re-suspended in 6H media, and then plated at a density of 10,000 cells/well to each of the eight outer wells of the disc, each of equal radial distance from the disc center. These wells are at the same location as previously stated (Figure 5). Using the wells with equal radial distance allowed for a constant oscillational acceleration between each well. Cells were allowed to adhere for 2 days before the media was replaced with 5H media. The wells were rinsed with PBS three times before being incubated with 5H media for another 48 hours. 2 m/s^2 was chosen for oscillational acceleration, as in the previous chapter.

Rho/ROCK Inhibition

Before FRTL-5 cells were exposed to vibratory stimulation, 330 μL of the 10 μM Y27632 (Sigma, Mo) was added to 4 of the 8 wells in the multi-well disc. Y27632 is a rho kinase inhibitor that interferes with ROCK activators (135). The 5H media was replaced in the other wells. 4 control well also received the same media as the multi-well disc without oscillation. Cells were exposed to a continuous 4 hours of oscillations at 2

m/s². The control plate was placed in the TRB warming chamber. Following the 4 hours in the TRB, metabolic activity was measured.

Actin Polymerization Inhibition

Following the 48 TSH deprivation, 330 μ L of 0.2 μ M cytochalasin D (Sigma, Mo) was added to half of the wells in the multi-well disc and half of the wells in the controls. Cytochalasin D prevents actin polymerization (136). The multi-well disc was connected to the TRB and subjected to a constant oscillation at 2 m/s². The control plate was placed in the warming chamber for the TRB.

Metabolic Activity Assay

Alamar Blue (alamarBlue®, Life Technologies, Grand Island, NY) was used to quantify differences in metabolic activity in response to exposure to TSH and oscillatory accelerations (89). A 10x stock solution of Alamar Blue was diluted in calcium and magnesium free PBS to achieve a 1x final concentration. At the conclusion of each experiment, medium was removed, the wells were washed gently with PBS, and 100 μ L of Alamar Blue solution was added to each well. Both the multi-well discs and controls were returned to the incubator for 1 hour. The Alamar Blue solution was then transferred to a black 96-well plate and the fluorescence was measured (Ex/Em = 560/590 nm) with a fluorometer (FLOUstar, BMG LABTECH Ltd., Ortenberg, Germany). Results are reported in arbitrary fluorescence units (AFU) with the blank value subtracted.

Cell Number Quantification

Hoechst 33342 (H1399, Life Technologies, Grand Island, NY) was used to quantify cellular DNA. After alamar blue was removed, the wells were washed with PBS and 100 μ L of 5 μ g/mL Hoechst in PBS was added to each well, followed by a 30 minutes incubation at 37 °C. Fluorescence was measured (Ex/Em = 380/460 nm) with a flourometer (FLOUstar, BMG LABTECH Ltd., Ortenberg, Germany) and reported as AFU.

Live/Dead

Live/Dead assay was used to determine cell death after oscillation with inhibitors. Immediately following oscillations, the media was removed, and ethidium homodimer and calcein AM were added at 2 mM and 4 mM concentrations in PBS. Cells were incubated at 37 degrees Celsius for 30 minutes. Following the incubation, fluorescent images were taken.

Statistical Analysis

All data are presented as mean values \pm standard deviation. The oscillation and TSH condition for the alamar blue and Hoechst assays represents n = 12 samples. One-way analysis of variance (ANOVA) with post hoc Tukey tests (Prism 7, GraphPad) were then used to determine statistical significance.

Results

Metabolic activity for FRTL-5 cells with inhibition of Rho/ROCK activity is displayed in Figure 12. The results are normalized to the metabolic activity of the controls with no hormone or mechanical stimulation. Exposure to 4 hours of 2 m/s^2 accelerations in the TRB increased the metabolic activity by $20.3 \% \pm 30.3$. FRTL-5 cells incubated with TSH had a $12.9 \% \pm 8.2$ increase in metabolic activity. Vibration of the FRTL-5 cells incubated with Y27632 and exposed to oscillational accelerations of 2 m/s^2 significantly increased their metabolic activity by $33.4 \% \pm 36.5 \%$ ($p = 0.0012$) over the control experiment.

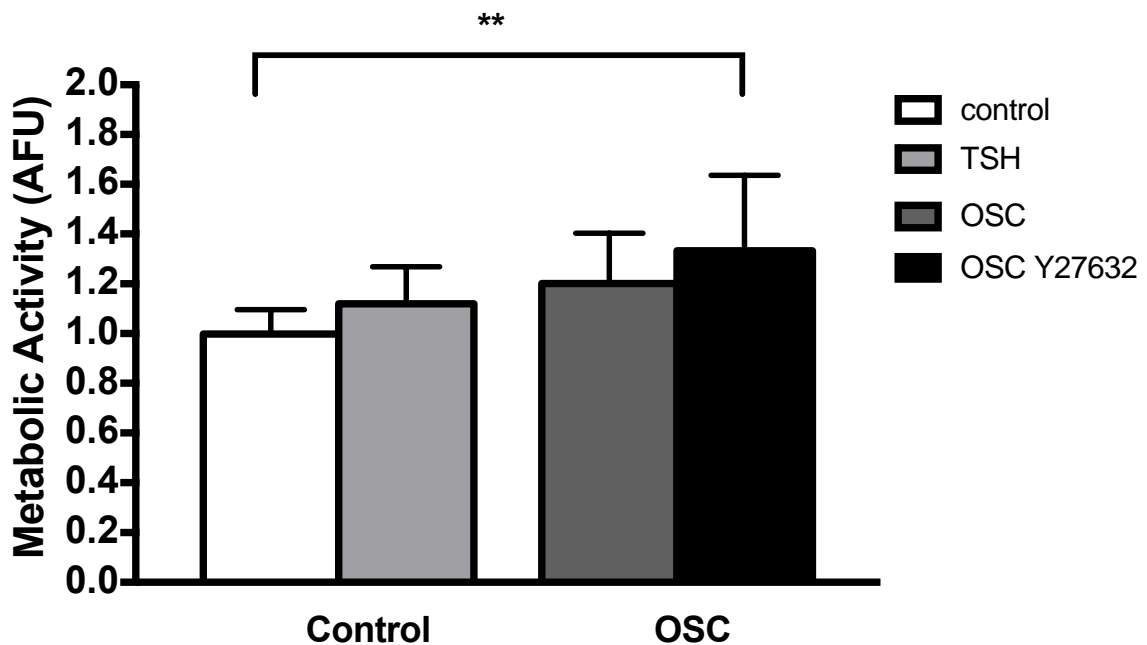


Figure 12. Metabolic activity increase by oscillation with Y27632 inhibition.

Inhibition of the Rho/Rock pathway in FRTL-5 cells did not change their metabolic response to oscillation when compared to previous results. Oscillation of FRTL-5 cells with Y27632 incubation increase metabolic activity by 33.4% ($p=0.0012$)

FRTL-5 metabolic activity was further assessed with the inhibition of actin polymerization (Figure 13). FRTL-5 cells metabolic activity was normalized to the control group of cells with no hormone or mechanical stimuli. Metabolic activity was increased significantly by $13.87\% \pm 7.4\%$ when FRTL-5 cells were exposed to 2 m/s^2 accelerations ($p=0.027$). When FRTL-5 cells were incubated with cytochalasin D and exposed to the TRB, metabolic activity modestly increased by $2.2\% \pm 16.5\%$, but was not significant compared to the control group. FRTL-5 cells metabolic activity was increased by $12.7\% \pm 17\%$ when incubated with 10 mU/mL of TSH and no exposure to vibration. There was no significance found between the control group and TSH or OSC plus cytochalasin D groups.

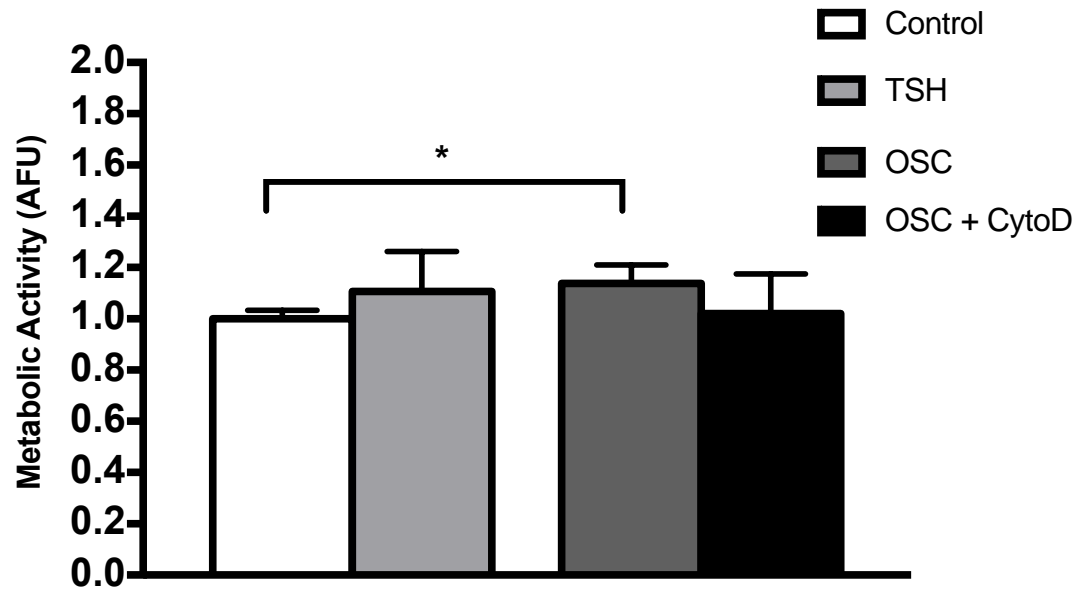


Figure 13. Oscillation does not increase metabolic activity when actin polymerization is inhibited. Inhibition of actin polymerization affects the FRTL-5 cells ability to sense the oscillation accelerations. There is no significant increase or decrease in metabolic activity. There was a significant increase in metabolic activity for oscillation alone ($p < 0.05$)

Live/Dead results indicated that cytochalasin D did not cause FRTL-5 cell death after vibration (Figure 14). Green indicates live cells and red color indicates dead cells. Metabolic activity was also measured on static FRTL-5 cells to verify cytochalasin D cytotoxicity levels and confirm that it did not inhibit metabolic activity.

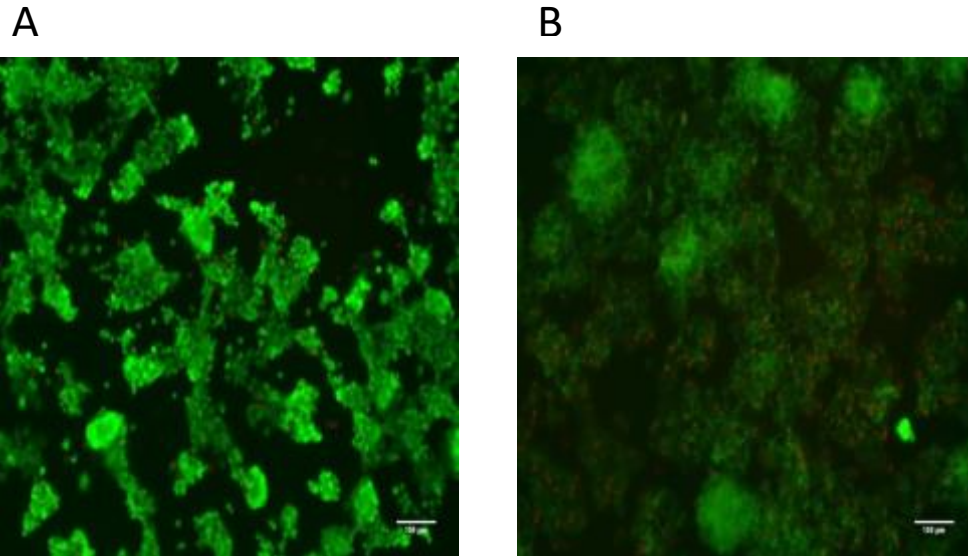


Figure 14. Live dead staining of FRTL_5 incubated with cytochalasin D.

Live/Dead staining was conducted after vibration of FRTL-5 cells to verify if cells were dying due to vibration and inhibition of actin polymerization (A) with TSH and (B) without TSH.

Incubation of FRTL-5 cells with Y27632 and cytochalasin D for 4 hours increased their metabolic activity by $9.7\% \pm 11.4$ and $5.1\% \pm 13.2$ (Figure 15). No significance was observed.

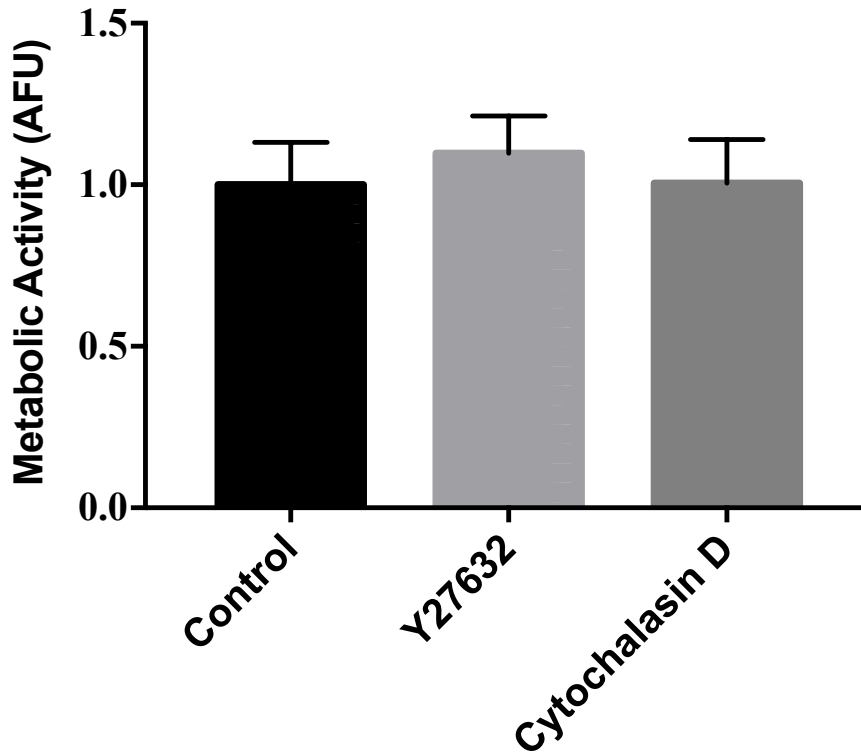


Figure 15. Verification that Y-27632 and cytochalasin D does not inhibit or increase FRTL-5 cells metabolic activity. Y-27632 and cytochalasin D inhibitors do not significantly increase or decrease metabolic activity.

Discussion

In chapter 2, I demonstrate that FRTL-5 cells responded to high frequency, small amplitude oscillations. Here, inhibition of actin polymerization interfered with the FRTL-5 cell's ability to sense the oscillation forces from the TRB. Inhibition of the Rho/ROCK pathway did not have the same effect. To verify that exposure to mechanical stimulation with these inhibitors did not cause cell death, the live/dead assay was conducted. The

assay verified that the cells were not dying due to vibration. However, cytochalasin D caused the cells to lose their rounded morphology.

Actin filaments are important for cell mechanosensing. These data show that disruption of the actin cytoskeleton also affects thyroid cell metabolism, and suggests that vibrational forces are providing mechanical cues to thyroid cells.

Chapter 4: Develop New Vibration Bioreactor for a more Physiological Environment

Introduction

To achieve a more physiological environment, I devised a voice coil bioreactor that can apply vibrational forces to FRTL-5 cells while in a temperature and CO₂ controlled environment. A CO₂-controlled environment is required for the pH of the culture medium (if bicarbonate buffered) to be maintained at 7.4. Environmental control will allow for longer than four hour duration experiments. The placement of the vibration device in an incubator also allows me to control the moisture. The inclusion of moisture and CO₂ have been shown to have positive effects on cellular behavior for longer duration experiments (137) . The TRB system only had temperature control, which limited experiments to four hours. The new bioreactor will greatly expand the duration of new experiments.

Material and Methods

Cell Culture

Fischer rat thyroid line cells (FRTL-5, ATCC) derived from the thyroid gland of Fischer rats were maintained in a 37 °C humidified incubator supplied with 95%/5% air/CO₂. FRTL-5 cells were cultured in modified Ham's F12 medium adjusted to contain 1.5 g/L sodium bicarbonate. Additional supplements were added to the medium: 1 mU/ml thyroid stimulating hormone (TSH), 0.01 mg/ml insulin, 10 nM hydrocortisone, 0.005 mg/ml transferrin, 10 ng/ml somatostatin, 10 ng/ml glycyl-L-histidyl-L-lysine acetate, 0.5

% bovine calf serum (Bidev 1984). Growth medium was used for cell expansion and to acclimate the cells prior to initiating acceleration experiments. Cells were passaged at 70% confluency and harvested at passages 4 to 8 for acceleration experiments. For acceleration experiments, growth medium was modified so that it either contained 10 mU/ml TSH or no TSH as noted below.

Voice Coil Bioreactor

A function generator was used to generate a sinusoidal wave form with an adjustable frequency and voltage output. A function generator (FeelTech, Korea) was placed outside of the incubator and connected to a loud speaker through speaker wire. The loud speaker provided the mechanical force to drive adherent cells with the desired oscillation characteristics. The speaker cone was completely removed to allow a 96-well plate to be attached to the speaker. The sink drain was centrally placed on the base of the speaker and adhered with double sided tape. The 96-well plate was attached to the sink drain. The voice coil bioreactor can be seen in Figure 16.

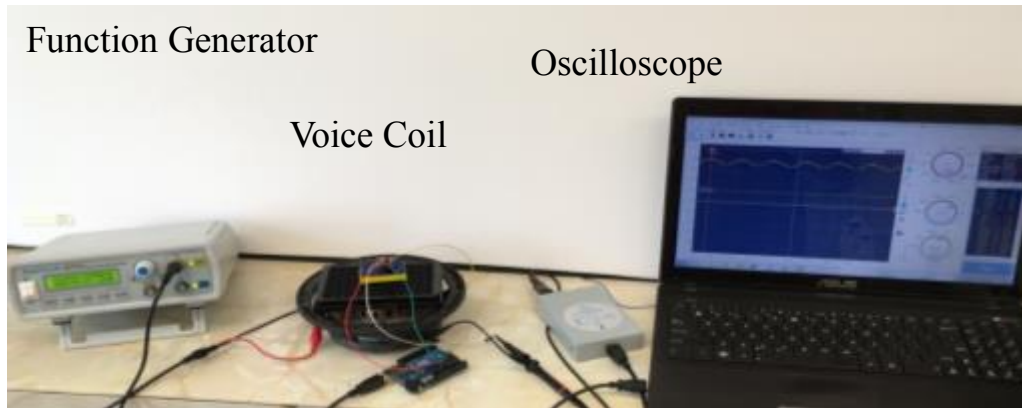


Figure 16. Voice coil bioreactor.

Acceleration Measurement

With the voice coil bioreactor, acceleration measurements were taken directly from the 96-well plate attached to the loud speaker. The voltage output on the function generator was adjusted until the desired acceleration was achieved. An ADXL335 analog accelerometer (Sparkfun, Boulder, CO) was used to determine the acceleration of the plate on the voice coil bioreactor. The accelerometer was placed on the plate containing the adherent cells. It was connected to a 3.3V power supply and had a constant 1.9V output under a 1g force. The output voltage from the accelerometer was collected to an oscilloscope. Software included with the oscilloscope was used to determine the peak to peak voltage. Oscilloscope data was compared with a Labquest 2 accelerometer and a hand held accelerometer (Benetech, Ca) with the capabilities to determine oscillational displacement. For experiments with FRTL-5 cells adhered to the 96-well plate, the ADXL335 accelerometer was placed on the top of the 96-well plate for measurement and verification of the acceleration. The voltage input on the function generator was adjusted until the correct acceleration was achieved. The results from the oscilloscope were displayed in peak to peak volts. The Labquest 2 measurements were graphed and a peak

to peak acceleration was recorded. The vibration amplitude measured from the handheld device was reported in millimeters.

Alamar Blue Assay

This assay is the same protocol from previous chapters.

Quantification of Cell Number

Hoechst 33342 (H1399, Life Technologies, Grand Island, NY) was used to quantify cell number. After removal of Alamar Blue, the wells were washed with PBS and 100 μL of 5 $\mu\text{g}/\text{mL}$ Hoechst in PBS was added to each well, followed by a 30 minutes incubation at 37 $^{\circ}\text{C}$. Fluorescence was measured with a flourometer (Ex/Em = 380/460 ηm) and reported as AFU.

Quantification of Reactive Oxygen Species (ROS) Levels

A dichlorofluorescein (DCF) assay (D399, ThermoFisher) was conducted on a separate set of experiments that were subjected to identical experimental conditions as those for the previous assay in order to measure differences in ROS production (90). After stimulation, media was removed from the wells and replaced with 50 μL of 10 μM DCF in PBS solution and incubated at 37 $^{\circ}\text{C}$ for 30 minutes. ROS production was measured with a fluorometer (Ex/Em = 495/520 nm) and reported as AFU.

Statistical Analysis

All data are presented as mean values \pm standard deviation. The oscillation and TSH condition for the alamar blue and Hoechst assays represents $n = 24$ samples. One-way analysis of variance (ANOVA) with post hoc Tukey tests (Prism 7, GraphPad) were then used to determine statistical significance.

Results

The first input condition with the function generator was a 40 Hz sinusoidal wave with a peak to peak voltage of 2V. The minimum acceleration from the collected data was 8.54 m/s^2 and a maximum acceleration of 10.49 m/s^2 for those given inputs (Figure 17). The max observed peak to peak acceleration was 1.95 m/s^2 . With the same conditions, the oscilloscope display generated wave form at 40 Hz and a peak to peak voltage of 0.045 V (Figure 18). The analog accelerometer was rated a 0.3 V/G, which gives a peak to peak acceleration of 1.47 m/s^2 . This procedure was repeated for a variety of additional input conditions. The acceleration results are shown in Table 1.

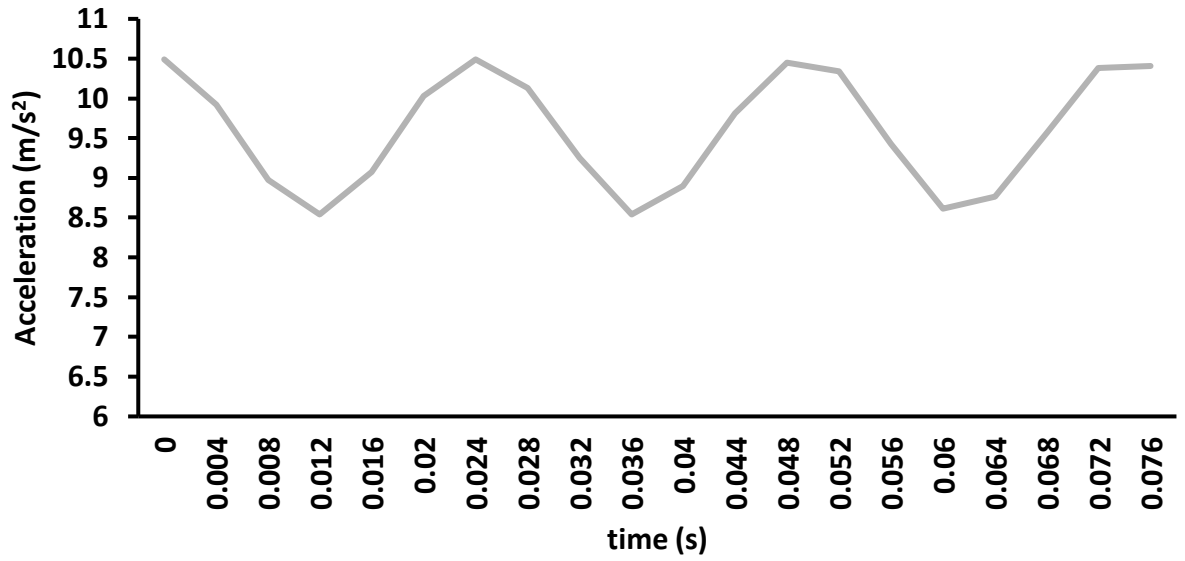


Figure 17. Labquest 2 data. Acceleration data was collected on the hand held labquest 2 accelerometer. The accelerations were graphed and the peak to peak value was determined for each given input values.

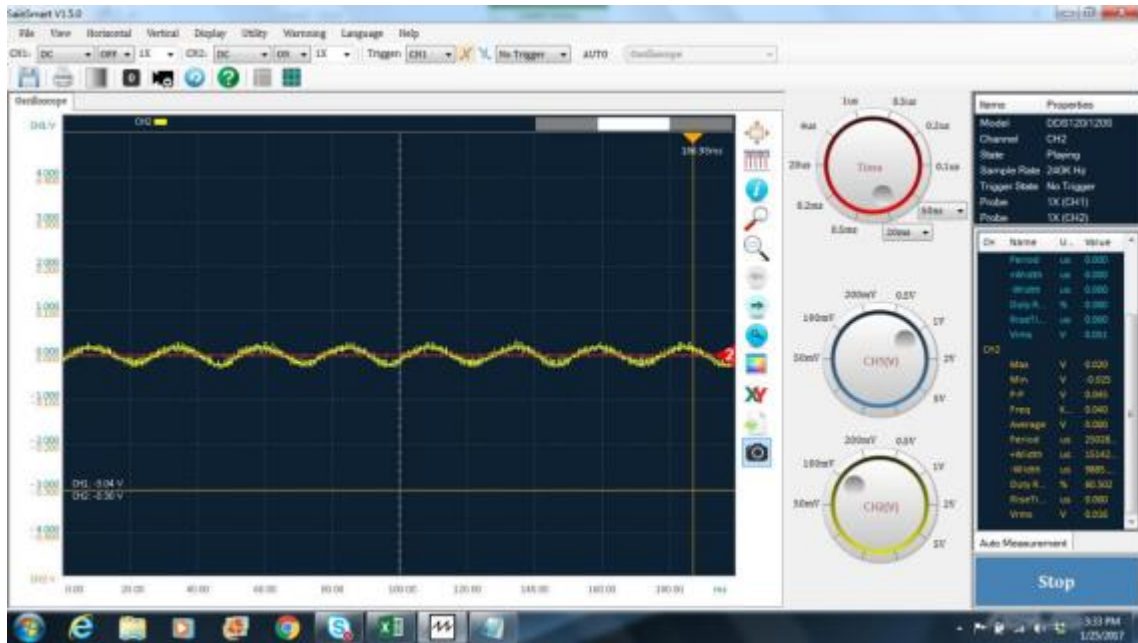


Figure 18. Screenshot of oscilloscope readout. When the oscilloscope is connected to vibrating accelerometer a voltage output waveform is created. The software gives frequency and peak to peak values of the waveform.

INPUT CONDITION (Frequency, Voltage)	LABQUEST 2 ACCELERATION (m/s²)	ANALOG ACCELERATION (m/s²)
40 Hz, 2V	3.0	1.5
40 Hz, 8V	8.5	6.7
40 Hz, 14V	13.9	11.1
60 Hz, 2V	12.0	11.4
60 Hz, 8V	37.2	36.0
126 Hz, 0.7V	2.4	2.1
126 Hz, 8V	27.5	22.6

Table 1. Acceleration reading from different function generator inputs.

Discrepancies between the two accelerometers was greatest at lower frequencies. As frequency increased, the difference in accelerations were reduced.

The percent difference between the two accelerometers was also calculated. The first function generator input of 40 Hz and 2V had a 104% difference between measurements. The input values of 40 Hz with 8V and 14V had differences of 27.3% and 25.7%, respectively. For a frequency of 60 Hz, input voltage potentials of 2V and 8V were chosen. Their corresponding acceleration from the two measuring devices had a difference of 5.2% and 3.44%. The last function generator input values considered were at 126 Hz with voltage potentials of 0.7V and 8V. The corresponding differences between accelerometer measurements were 14.3% and 21.7%, respectively.

The acceleration was also measured with a handheld accelerometer. This device could display the displacement caused by the oscillation of the loud speaker. Similar input condition for the function generator were chosen to verify the accuracy of the ADXL 335 analog accelerometer against the handheld accelerometer. The input frequencies were 60, 126, and 160 Hz with voltage inputs of 1, 2, 3, and 5V. The corresponding accelerations were calculated using the conversion of 0.3V is equal to 1G for the ADXL 335 accelerometer. Equation 1 was used to determine the acceleration from the displacement values. The displacements and the corresponding accelerations are shown in Table 2. The peak to peak voltage is also shown to verify the accuracy of the ADXL 335 accelerometer. Table 3 shows the acceleration comparison between the two devices.

Input Voltage	P-P (V)	Acceleration (m/s ²)	d (mm)	Acceleration (m/s ²)	% difference
1	0.07	2.29	0.02	2.83	24%
2	0.164	5.36	0.03	4.26	20.5%
3	0.327	10.69	0.06	8.5	20.3%
5	1.21	39.5	0.25	35.5	10.1%

Table 2. Comparison of ADXL 335 and the handheld accelerometer at 60 Hz. The function generator was set to 60 Hz and a range of voltage potential was set form 1V to 5V. A 1V input showed a 24% difference. 2V and 3V inputs had a difference of 20.5% and 20.3%.

Input Voltage	P-P (V)	Acceleration (m/s ²)	d (mm)	Acceleration (m/s ²)	% difference
1	0.104	3.4	0.01	6.25	16.7%
2	0.174	5.69	0.01	6.25	25.1%
3	0.2	6.54	0.01	6.25	4.4%
5	0.257	8.4	0.02	12.5	50%

Table 3. Comparison of ADXL 335 and the handheld accelerometer at 126 Hz.

Input Voltage	P-P (V)	Acceleration (m/s ²)	d (mm)	Acceleration (m/s ²)	% difference
1	0.164	5.36	0.01	10.08	88%
2	0.374	12.23	0.01	10.08	17.6%
3	0.421	13.76	0.01	10.08	26.7%
5	0.491	16.01	0.02	20.16	25.9%

Table 4. Comparison of ADXL 335 and the handheld accelerometer at 160 Hz.

Metabolic activity was measured from FRTL-5 cells using the voice coil bioreactor (Figure 17). FRTL-5 cells exposed to vibration had an increase in metabolic activity by 24% without TSH in the media and 28% with 10 mU/mL TSH in the media. The metabolic activity results from the voice coil bioreactor were compared with the metabolic activity results from the TRB in chapter 2 (Table 5). TSH had the same metabolic increase over the controls as the previous TRB experiments. Metabolic activity, after oscillation in the voice coil bioreactor, increase 2% when compared to the metabolic increase from oscillation in the TRB. Oscillation with the addition of TSH decreased 11% when compared to the TRB results.

	TRB	Voice coil	Percent Difference
NO TSH, NO Oscillation	1.00 ± 0.13	1.00 ± 0.26	0%
TSH, No Oscillation	1.11 ± 0.17	1.11 ± 0.25	0%
No TSH, Oscillation	1.19 ± 0.15	1.21 ± 0.22	1.6%
TSH, Oscillation	1.33 ± 0.09	1.2 ± 0.19	9.7%

Table 5. Comparison of FRTL-5 cell metabolic activity after vibration with TRB or voice coil bioreactor.

ROS was measured after FRTL-5 cells were exposed to oscillational accelerations of 2 m/s² in the voice coil bioreactor (Figure 18). ROS increased by 16.54% when FRTL-5 cells were exposed to 10 mU/mL of TSH. ROS also increased by 14.1% and 22.9% when FRTL-5 cells were exposed to oscillation and oscillation plus TSH.

These results were also compared to previous ROS production when cells were exposed to oscillations in the TRB from Chapter 2 (Table 6). ROS production jumped by 6 percent from previous experiments with TSH activation. However, ROS production in the voice coil bioreactor system shows a decline when compared to the TRB system. ROS was decreased by 10% and 14% when exposed to oscillation and oscillation with TSH in the voice coil system.

	TRB	Voice coil	Percent difference
No TSH, No Oscillation	1.00 ± 0.11	0.97 ± 0.18	3%
TSH, No Oscillation	1.10 ± 0.23	1.16 ± 0.21	5.4%
No TSH, Oscillation	1.24 ± 0.17	1.14 ± 0.23	8%
TSH, Oscillation	1.36 ± 0.27	1.22 ± 0.25	10.3%

Table 6. Comparison of ROS activity with the TRB and voice coil system.

Discussion

The work in this chapter aimed to develop a new device to apply oscillational acceleration to adherent cells in a 96-well plate under more controlled environmental conditions. To achieve the desired accelerations at a frequency similar to human speech, a loud speaker was chosen. The loud speaker was driven by a function generator capable of producing the desired frequencies and a changeable voltage potential. One main concern with this design was the ability of the speaker to drive the weight of the plate and liquid in the plate at our desired accelerations. Initial experiments showed that accelerations of 2 m/s² were easily achievable with this system. We were able to achieve acceleration around 30 m/s² with an input of 8V from the function generator. The maximum voltage potential of the function generator is 20V.

The development of the voice coil bioreactor allowed me to better control the surrounding FRTL-5 environment. However, I did lose some accuracy in specifying the oscillational forces applied, and in the driving force capabilities compared to the TRB.

The ADXL 355 did not work very well at lower frequencies, but did have a high enough sampling rate when connected to an oscilloscope to produce a precise waveform. A limited sampling rate was the main problem with the labquest 2 accelerometer. I could not get a high enough sampling rate to produce a correct waveform at 126 Hz. The main concern with of using the hand held devices was the fear of damping the vibrational forces. Damping was observed when the ADXL 335 was connected a plate and the hand held accelerometer was placed on the plate for a reading. A noticeable drop in the signal was detected, but a reading from both dampened signals was able to be read. When all these devices data were collected and analyzed, we were able to show that we can measure the acceleration of the 96 well plate at high frequencies and small amplitudes.

Once we verified we could measure the acceleration, it was important to compare the TRB results with the voice coil bioreactor results. The data indicate that the voice coil bioreactor is capable of inducing a similar metabolic response from FRTL-5 cells as the TRB. It was a concern, given the different vibration motions is now in an up and down motion (Figure 19), as opposed to, the rotational motion of the TRB. We also verified that ROS production was increased when oscillational accelerations were applied in the voice coil bioreactor. Our results show that ROS is increased, although, not as much as with the TRB.

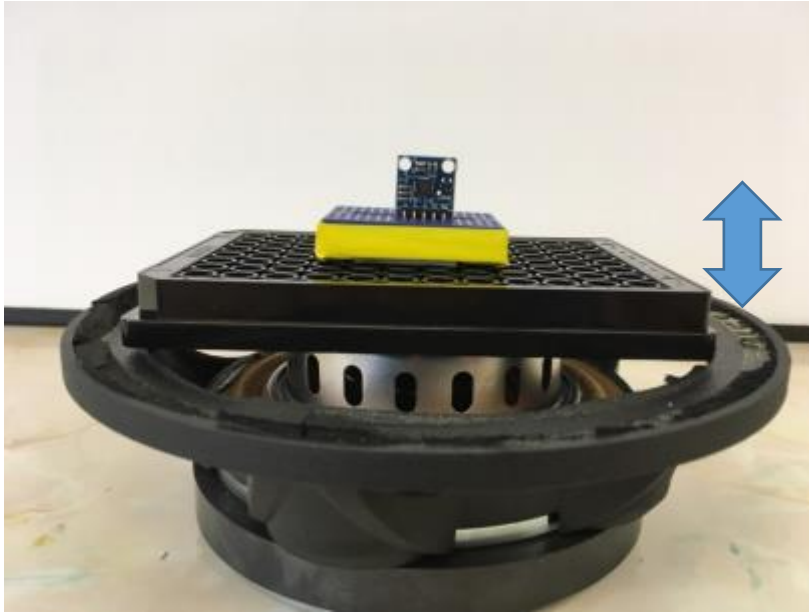


Figure 19. Motion created by voice coil.

Chapter 5: Evaluate Aim 3: Cellular Response to Vibratory Stimulation in a Dose Dependent Manner

Introduction

Human speech is produced by two vocal cords colliding with great oscillational accelerations. This force created by the vocal cords is transmitted to and dissipated by the surrounding tissue. The energy we previously use is in the form of vibrations at 126 Hz with an acceleration of 2 m/s^2 . Whereas this is insightful information, the amount of energy created by the vocal cords vary widely (in the form of oscillational frequency and amplitude) (64). We also had the FRTL-5 cells exposed to a constant vibration. To better understand a physiological response, we needed to adjust some of the parameters. This chapter looks at FRTL-5 cells response to vibrations with increased accelerations and different duty cycles.

Vibrational dosage has been shown to have an important effect on biological systems. Studies have shown that, while squatting on a vibrating plate, increasing the dosage increases the physiological response (138). However, this dosage increase also has been shown to increase negative effects associated with excessive vibrations (139). This is of concern in our system because of hydrogen peroxide, a vital part of making thyroid hormone, has been shown to increase with vibration (125). An increase in hydrogen peroxide is an area of concern, because it is associated with increased oxidative stress and might be correlated to thyroid disease (8, 14, 15).

Material and Methods

Cell Culture

Fischer rat thyroid line cells (FRTL-5, American Type Culture Collection, Rockville, MD, CRL 8305) derived from the normal thyroid gland of Fischer rats were maintained in a 37 °C humidified incubator supplied with 95%/5% air/CO₂. FRTL-5 cells were cultured according to the supplier's recommendations in Ham's F12K medium with 2 mM L-glutamine and adjusted to contain 1.5 g/L sodium bicarbonate. 0.5% bovine calf serum and six additional hormones required for FRTL-5 cells to proliferate and maintain thyroid function were added to the medium, as specified by the originators of this cell line (79, 80). These six hormones included 1 mU/ml thyroid stimulating hormone (TSH), 0.01 mg/ml insulin, 10 nM hydrocortisone, 0.005 mg/ml transferrin, 10 ng/ml somatostatin, and 10 ng/ml glycyl-L-histidyl-L-lysine acetate (All reagents from Sigma, St Louis, MO) (81). Growth medium was used for cell expansion and to acclimate the cells prior to initiating the experiments. For the experiments, growth medium was modified so that it either contained 10 mU/ml TSH or no TSH as indicated below. Cells were passaged at 70% confluency and harvested at passages four through eight for the experiments.

Voice Coil Bioreactor

FRTL- 5 cells were seeded in the center of a 96-well plate at a density of 10,000 cells/well. Cells were allowed to adhere for 48 hours in 6H media. After the initial 48 hours of incubation, the 6H media was removed. Each well was wash 3 times with PBS. Following the last PBS wash, FRTL-5 cells were cultured in 5H media for another 48 hours. After the TSH deprivation, 5H media was replaced in half of the wells and the other half received media with 10 mU/mL TSH. The 96-well plate was then attached to the loud speaker and the desired frequency was entered into the function generator. With the ADXL 335 accelerometer attached to the top of the plate, the voltage input on the function generator was adjusted until the correct acceleration was achieved.

Duty Cycle Analysis

Once attached to the loud speaker, the 96-well plate was exposed to two different on/off cycles. The first set of vibration cycles were varied between 2 m/s^2 and no oscillation for a total of four hours. The cycle would start with vibration for one hour and then with no movement for the next hour. This was repeated one more time. For the second condition, the same duty cycle was conducted but with a different starting condition (no oscillation/oscillation). The ADXL 335 accelerometer was attached the top of the plate and used verify an acceleration of 2 m/s^2 .

Dosage Effects

FRTL-5 Cells were culture in T-25 flask until 70% confluence. After they reach 70% confluence, they were passaged with trypsin/EDTA and seeded at a density of

10,000 cells/well. They were seeded in a 96 well plate in centrally located wells. The plate was then fixed to the loud speaker to allow for mechanical stimulation. Oscillational accelerations were set for 2, 4, and 6 m/s². The input voltage on the function generator was varied until a corresponding peak to peak voltage from the ADXL 335 accelerometer was achieved to match the desired accelerations. The experiment was carried out for a time duration of 4 hours.

Quantification of Metabolic Activity

Alamar Blue (AlamarBlue®, Life Technologies, Grand Island, NY) was used to quantify differences in metabolic activity in response to exposure to TSH and oscillatory accelerations (89). A 10x stock solution of Alamar Blue was diluted in calcium and magnesium free PBS to achieve a 1x final concentration. At the conclusion of each experiment, medium was removed, the wells were each washed gently with PBS, and 100 µL of Alamar Blue solution was added to each well. Both the multi-well discs and controls were returned to the incubator for 1 hour. The Alamar Blue solution was then transferred to a black 96-well plate and the fluorescence was measured (Ex/Em = 560/590 nm) with a fluorometer (FLOUstar, BMG LABTECH Ltd., Ortenberg, Germany). Results are reported in arbitrary fluorescence units (AFU) with the blank value subtracted.

Quantification of Cell Number

Hoechst 33342 (H1399, Life Technologies, Grand Island, NY) was used to quantify cell number. After removal of Alamar Blue, the wells were washed with PBS and 100 μ L of 5 μ g/mL Hoechst in PBS was added to each well, followed by a 30 minutes incubation at 37 °C. Fluorescence was measured with a flourometer (Ex/Em = 380/460 nm) and reported as AFU.

Quantification of Reactive Oxygen Species (ROS) Levels

A dichlorofluorescein (DCF) assay (D399, ThermoFisher) was conducted on a separate set of experiments that were subjected to identical experimental conditions as those for the previous assay in order to measure differences in ROS production (90). After stimulation, media was removed from the wells and replaced with 50 μ L of 10 μ M DCF in PBS solution and incubated at 37 °C for 30 minutes. ROS production was measured with a fluorometer (Ex/Em = 495/520 nm) and reported as AFU.

Statistical Analysis

All data are presented as mean values \pm standard deviation. The oscillation and TSH condition for the alamar blue, ROS and Hoechst assays represents n = 24 samples. One-way analysis of variance (ANOVA) with post hoc Tukey tests (Prism 7, GraphPad) were then used to determine statistical significance.

Results

Metabolic activity was measured in FRTL-5 cells with a varying vibration sequence. Oscillation or static conditions always last for one hour. One of the conditions starts with oscillation (Figure 20) and the other condition starts in with no oscillation (Figure 21). When the FRTL-5 cycle ended with the static condition, the metabolic activity decreased by 7.1%. TSH increased the metabolic activity by 6.3% and 3.6% when FRTL-5 were also incubated with TSH during oscillation. However, when FRTL-5 cells ended the cycle with oscillation, their metabolic activity increased to similar levels as 4 hours of constant oscillation. Metabolic activity was increased by 28.6% when cells ended with oscillation. The increase jumped by 46.1% with oscillation at 2 m/s² and incubation of TSH.

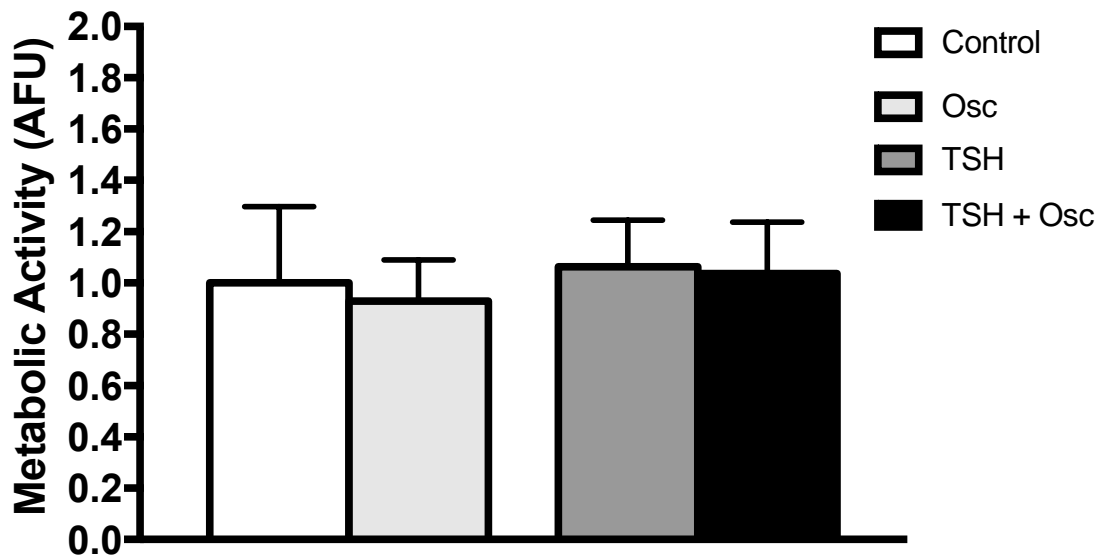


Figure 20. Metabolic activity of FRTL-5 cells with a 1-hour vibration/ 1-hour static ratio for 4 hours.

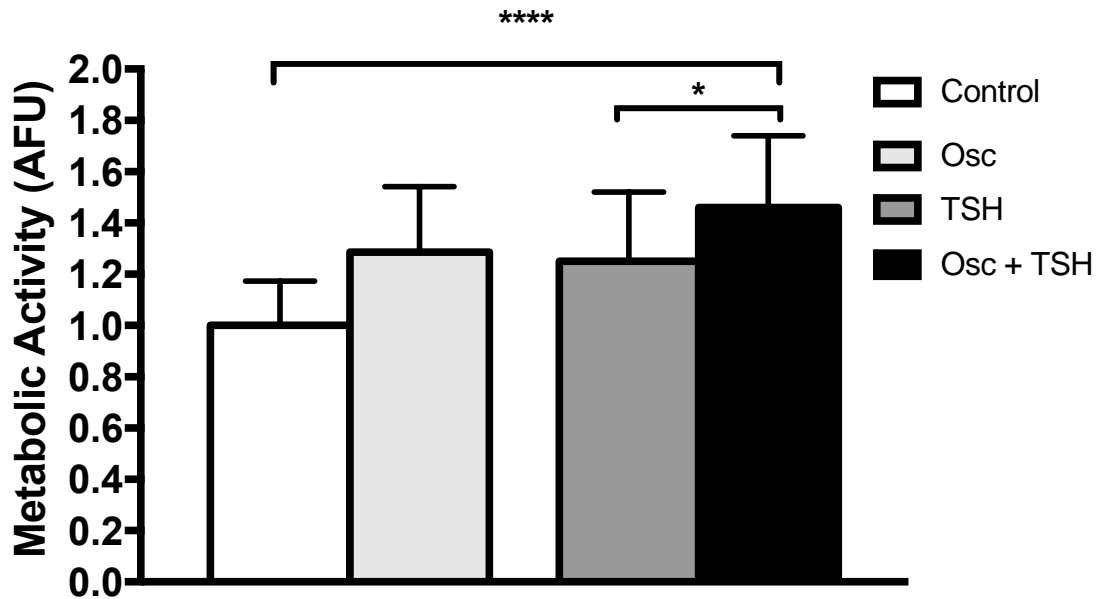


Figure 21. Metabolic activity of FRTL-5 cells with a 1-hour static/ 1-hour vibration ratio for 4 hours. Oscillation plus TSH showed the largest increase and significance over the control groups ($p < 0.0001$). This group also had a significance increase over the TSH activated group ($p < 0.05$).

Metabolic Activity was also measure with an increasing acceleration (Figure 22). FRTL-5 cells were exposed to accelerations of 2, 4, and 6 m/s^2 . The corresponding accelerations had increases in metabolic activity of $19\% \pm 22.7$, $32.9\% \pm 30.0$, and $29\% \pm 24.8$ for cells vibrated without TSH in the media. Metabolic activity increased by $33\% \pm 25$, $36\% \pm 36$, and $29\% \pm 21$ with exposed to media with 10 mU/mL TSH and vibration at the given accelerations.

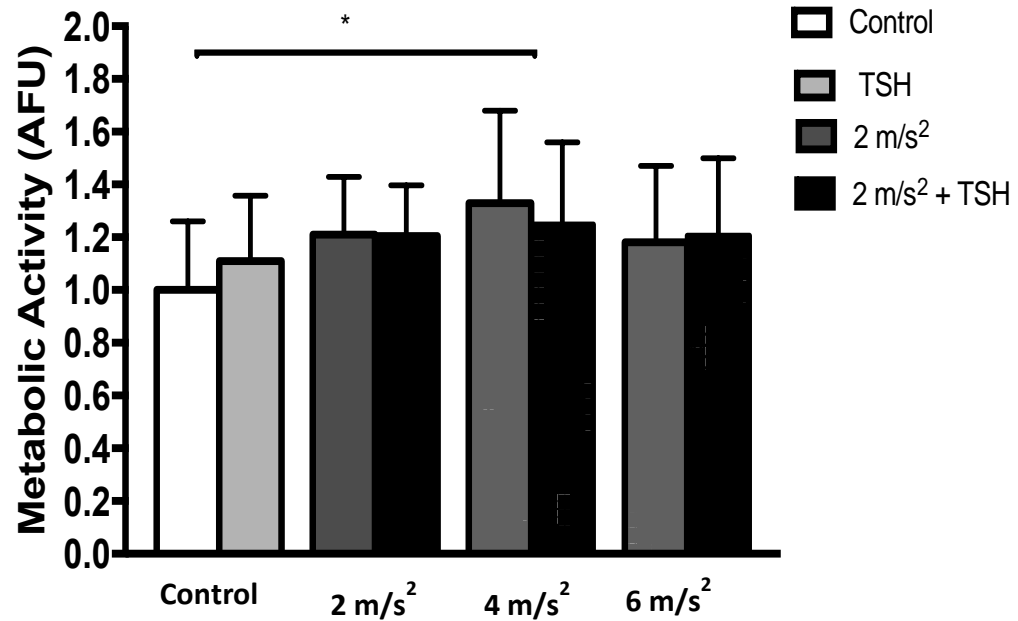


Figure 22. Metabolic activity at various accelerations. Accelerations at 4 m/s² shows a significant increase over control groups ($p < 0.05$).

Cellular detachment from oscillation was also measured (Figure 23). Oscillation at 2 m/s² had a decrease in cellular DNA of $0.47\% \pm 17.3$ as compared to the controls. At 4 m/s², the DNA loss jumped to $3.314\% \pm 22.1$, and oscillation at 6 m/s² had a decrease of DNA of 0.74 ± 25.2 .

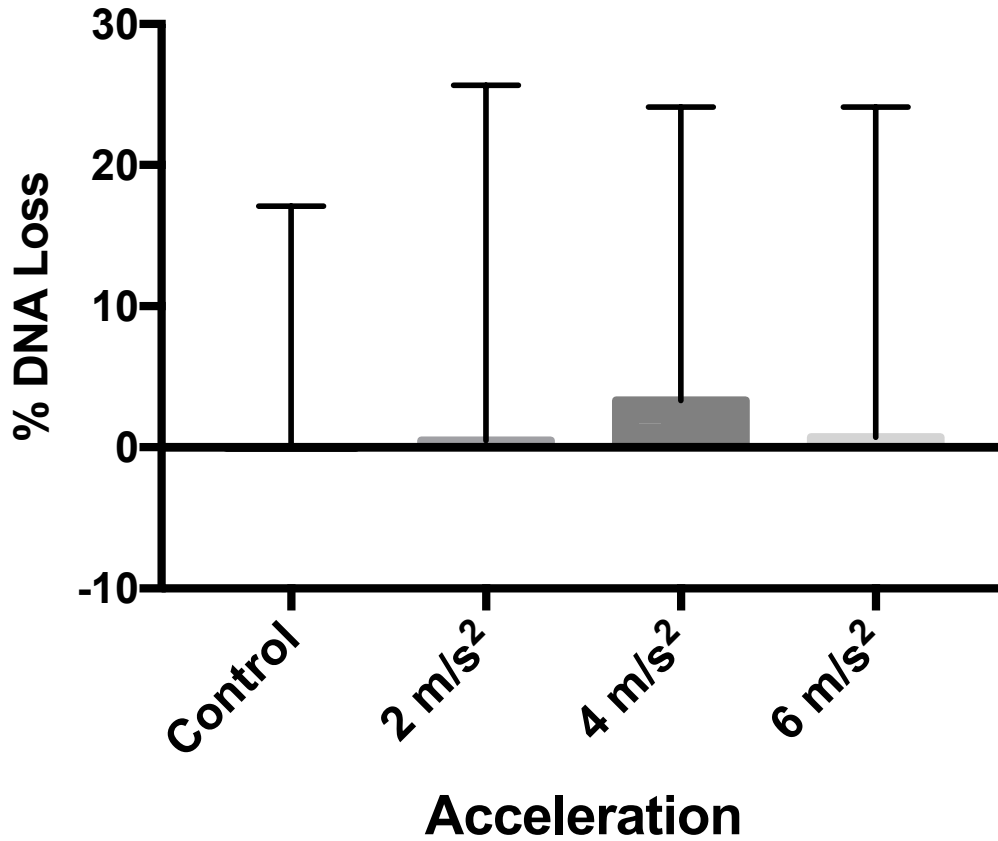


Figure 23. DNA loss due to oscillation. DNA content of the well decreased slightly from control value for each oscillational accelerations condition. 4 m/s² showed the largest decrease of 3.314%. There was no significance between any of the groups.

ROS activity was measured with the various accelerations as previously stated (Figure 24). At oscillational acceleration of 2 m/s² total ROS increased by 14% ± 23 (p < 0.05) and 22% ± 25.4 (p < .01) when FRTL-5 were incubated with 10 mU/mL of TSH along with oscillation. ROS activity was further increased by 32.09% ± 29.8 (p < .01) when exposed to oscillational accelerations of 4 m/s². However, when FRTL-5 cells were oscillated at 4 m/s² and incubated with TSH, the ROS activity only increased by 21.5% ± 32. ROS activity was also measured at oscillations acceleration of 6 m/s² and showed an

increase of $57.84\% \pm 22$ ($p < 0.001$). ROS was also increased by $55.54\% \pm 36.1$ ($p < 0.001$) when FRTL-5 cells were stimulated by TSH and oscillation.

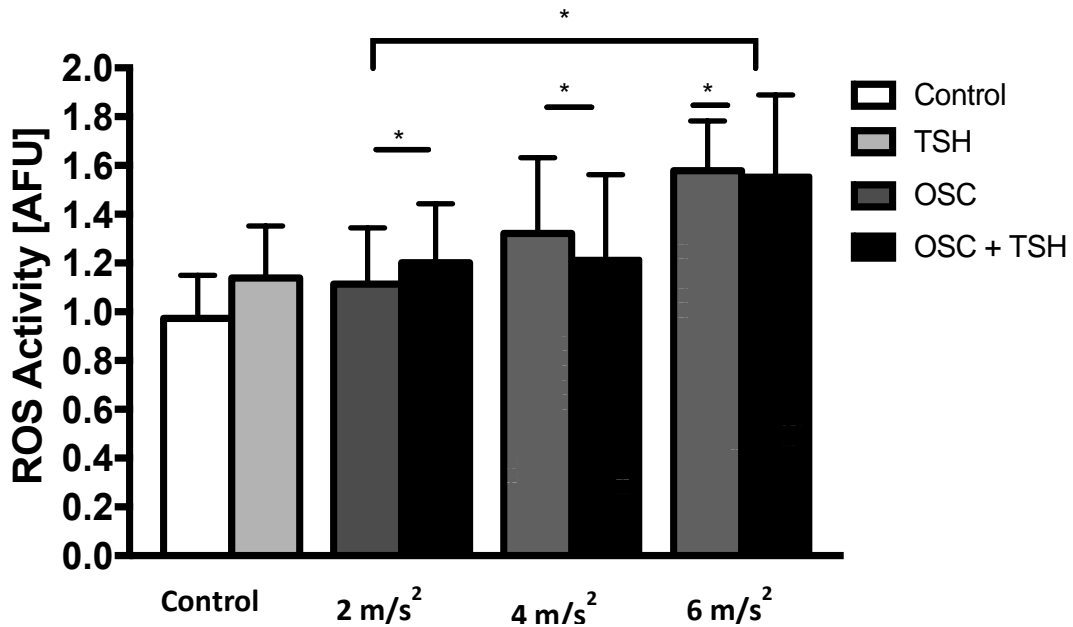


Figure 24. ROS at various accelerations. ROS was shown to increase with every conditions. The 6 m/s² accelerations were also significantly higher than the 2 m/s².

Discussion and Conclusion

Given that the thyroid is not constantly exposed to vibrations (our previous work was conducted at a constant 4 hour vibration), it was important to vary oscillation conditions with static conditions. Data from this chapter demonstrate thyroid cells ability to normalize their metabolic activity back to a control level after exposure to oscillation. Results also showed, when cells were exposed to oscillation/static/oscillation, thyroid cells were not damaged by the previous oscillation exposure and could respond with an increase in metabolic activity after a static condition.

Since it is not exactly known how much vibrational forces are transmitted to the thyroid from vocalization, a range of accelerations was useful in determining if the metabolic response of FRTL-5 thyroid cells would increase with increasing oscillational accelerations. Increasing the acceleration from 2 to 4 m/s² did increase metabolic activity. But, this trend did not continue as the accelerations increased to 6 m/s². This may have been due to the cells be damaged at higher accelerations or the potential for cell loss with the increasing accelerations. When looking at the percentage of DNA lost due to oscillation exposure, it is fairly clear that significant amount of cells were not detaching from the plate due to these forces. However, we did have each well completely filled with media to minimize the fluid shear stresses (110). The cellular loss could potentially be greater in a higher shear stress environment. The fact that cell loss is roughly the same for all acceleration conditions lead us to believe that FRTL-5 cells metabolic activity is increased due to increasing oscillation accelerations. However, this was not true for the highest acceleration of 6 m/s². The decrease in metabolic activity from 4 m/s² to 6 m/s² may be due to an increase in cellular stress at higher accelerations. We also noticed that accelerations of 4 m/s² had the largest percent of DNA loss. Since all the metabolic activity data from each are divided by the total DNA in that same well, the measured loss of DNA could have inflated the metabolic activity/DNA results shown for the 4 m/s² data. With that being said, each of the conditions still had an increase in metabolic activity due to oscillation.

An increase in vibratory oscillation is usually associated with certain risk factors (140). For this study, we investigated ROS levels since there is concern with hydrogen peroxide, an ROS, and thyroid health (15). Our studies showed that ROS was increased

with an increasing acceleration. This is of concern given the negative effects of excessive ROS generation, but thyroid cells need hydrogen peroxide and are able to handle normal physiological amounts of ROS (141). An interesting result from the data is the fact that ROS activity was decreased in the 4 m/s² and 6 m/s² experiments when thyroid cells were incubated with TSH. This may be due to an increase in antioxidants caused by TSH stimulation of thyroid cells (142).

Chapter 6. Future Work and Discussion

Introduction

Extracellular matrix proteins (ECM) are natural supports for epithelial cells. It has been shown that many epithelial cells behave differently when cultured on ECM proteins as compared to tissue culture polystyrene (143). One of the main differences noticed is the ability of epithelial cells to form follicles (144). *In vivo*, thyroid cells are organized in follicles (Figure 25).

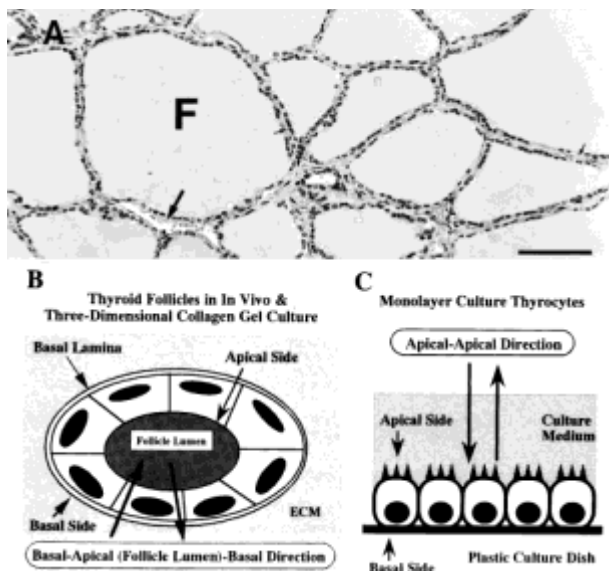


Figure 25. Thyroid follicles (142). (A) Thyroid histology. The round follicle can be seen the center lumen. (B) Polarity of thyroid cell in follicle orientation. (C) Thyroid cell orientation cultured on tissue culture polystyrene.

It is important to note, though it is generally considered to be positive when cells are cultured on a more physiological substrate, a disruption in the ECM could also be damaging to the adherent cells. This is seen in the thyroid with an increase in thyroid cancer when the ECM of thyroid tissue stiffens (145).

In this chapter, I will propose experimental procedures and report preliminary findings of future possible work. This will include culturing FRTL-5 cells on different ECM proteins and evaluate how they respond to static and dynamic conditions.

Material and Methods

Cell Culture

Fischer rat thyroid line cells (FRTL-5, American Type Culture Collection, Rockville, MD, CRL 8305) derived from the normal thyroid gland of Fischer rats were maintained in a 37 °C humidified incubator supplied with 95%/5% air/CO₂. FRTL-5 cells were cultured according to the supplier's recommendations in Ham's F12 medium with 2 mM L-glutamine and adjusted to contain 1.5 g/L sodium bicarbonate. 0.5% bovine calf serum and six additional hormones required for FRTL-5 cells to proliferate and maintain thyroid function were added to the medium, as specified by the originators of this cell line (79, 80). These six hormones included 1 mU/ml thyroid stimulating hormone (TSH), 0.01 mg/ml insulin, 10 nM hydrocortisone, 0.005 mg/ml transferrin, 10 ng/ml somatostatin, and 10 ng/ml glycyl-L-histidyl-L-lysine acetate (All reagents from Sigma, St Louis, MO) (81). Growth medium was used for cell expansion and to acclimate the cells prior to initiating the experiments. For the experiments, growth medium was

modified so that it either contained 10 mU/ml TSH or no TSH as indicated below. Cells were passaged at 70% confluency and harvested at passages four through eight for the experiments.

Application of Basement Membranes

Individual wells of a 96 well plate were coated with different proteins before FRTL-5 adhesion. Collagen type I was used at a concentration of 0.045 mg/mL. 200 μ L of the collagen type I solution was placed in each appropriate well. The collagen solution was allowed to adhere to the bottom of each well for 30 minutes at 37 degrees Celsius. Following the protein adsorption, FRTL-5 cells were seeded on top of the gel at a concentration of 10,000 cells per well. A basement membrane (BM, Sigma, St. Louis, Mo) solution was also used. 20 μ L of BM solution was added to each specified well of a 96-well plate. The BM gel was allowed to polymerize for 30 minutes at 37 degrees Celsius. After polymerization, FRTL-5 cells were added on top of the BM at a concentration of 10,000 cells per well.

Application of Vibrations with a Voice Coil Bioreactor

FRTL-5 cells were exposed to oscillational accelerations of 2 m/s² in the voice coil bioreactor for a duration of 4 hours. FRTL-5 cells were removed from T-Flask using trypsin and seeding in the appropriate wells of a 96-well plate. Cells were allowed to adhere for 48 hours before media was replaced with 5H media. FRTL-5 were cultured in 5H media for 48 hours to maximize their hormonal stimulation. After 48 hours, media was either replaced with 5H media or with media containing 10 mU/mL of TSH. One plate is used for the control and the other is placed on the loud speaker for mechanical

stimulation. The input voltage on the function generator was adjusted until the ADXL 335 accelerometer gave a peak to peak output voltage of 60 mV.

Quantification of Metabolic Activity

Alamar Blue (alamarBlue®, Life Technologies, Grand Island, NY) was used to quantify differences in metabolic activity in response to exposure to TSH and oscillatory accelerations (89). A 10x stock solution of Alamar Blue was diluted in calcium and magnesium free PBS to achieve a 1x final concentration. At the conclusion of each experiment, medium was removed, the wells were washed gently with PBS, and 100 μ L of Alamar Blue solution was added to each well. Both the multi-well discs and controls were returned to the incubator for 1 hour. The Alamar Blue solution was then transferred to a black 96-well plate and the fluorescence was measured (Ex/Em = 560/590 nm) with a fluorometer (FLOUstar, BMG LABTECH Ltd., Ortenberg, Germany). Results are reported in arbitrary fluorescence units (AFU) with the blank value subtracted.

Quantification of Cell Number

Hoechst 33342 (H1399, Life Technologies, Grand Island, NY) was used to quantify cell number. After removal of Alamar Blue, the wells were washed with PBS and 100 μ L of 5 μ g/mL Hoechst in PBS was added to each well, followed by a 30 minutes incubation at 37 °C. Fluorescence was measured with a fluorometer (Ex/Em = 380/460 nm) and reported as AFU.

Cell Morphology

FRTL-5 cells were cultured on TCPS for 2 days in 6H media. Following the 2 days, 6H media was replaced with 5H media. FRTL-5 cells were cultured for another 4 days with 5H media. The 5H media was replaced after 2 days. Following TSH deprivation for 5 day, FRTL-5 cells were either exposed to oscillation at 1 m/s^2 or TSH was reintroduced into the media at 1 mU/mL .

Statistical Analysis

All data are presented as mean values \pm standard deviation. The oscillation and TSH condition for the alamar blue and Hoechst assays represents $n = 4$ samples. One-way analysis of variance (ANOVA) with post hoc Tukey tests (Prism 7, GraphPad) were then used to determine statistical significance.

Results

Initial Results show that FRTL-5 cells have a different morphological appearance when cultured on different ECM proteins (Figure 26). For all previous experiments in this dissertation, FRTL-5 cells were cultured on tissue culture polystyrene. The images presented here show clear difference in cellular morphology. On tissue culture polystyrene the cells have distinct round edges and tend to grow on top of each other. On BM, FRTL-5 cells appear to form a sheet with very few cells growing in a 3-D structure. FRTL-5 cells cultured on collagen type I appear be growing in 3-D cluster.

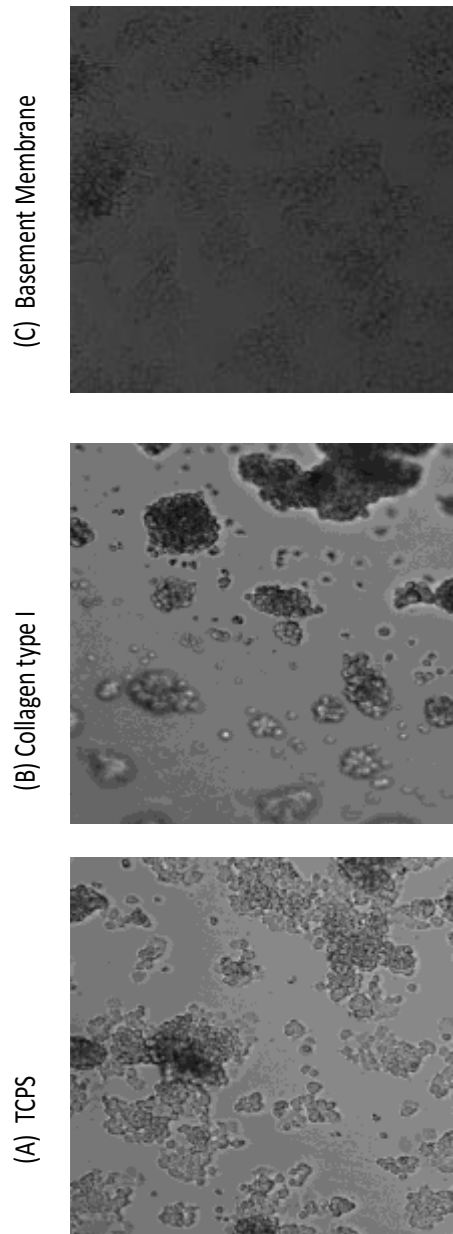


Figure 26. FRTL-5 cells cultured on (A) tissue culture polystyrene (B) collagen type I and (C) basement membrane.

Metabolic activity was measured for FRTL-5 cells cultured on collagen type I and exposed to TSH and or oscillation (Figure 27). Metabolic activity increase by $8.7\% \pm 19.2$ when exposed to 2 m/s^2 accelerations. An increase of 17.47 ± 18 was observed when cells were exposed to TSH and OSC. TSH induced and increase of $6.3\% \pm 16.3$.

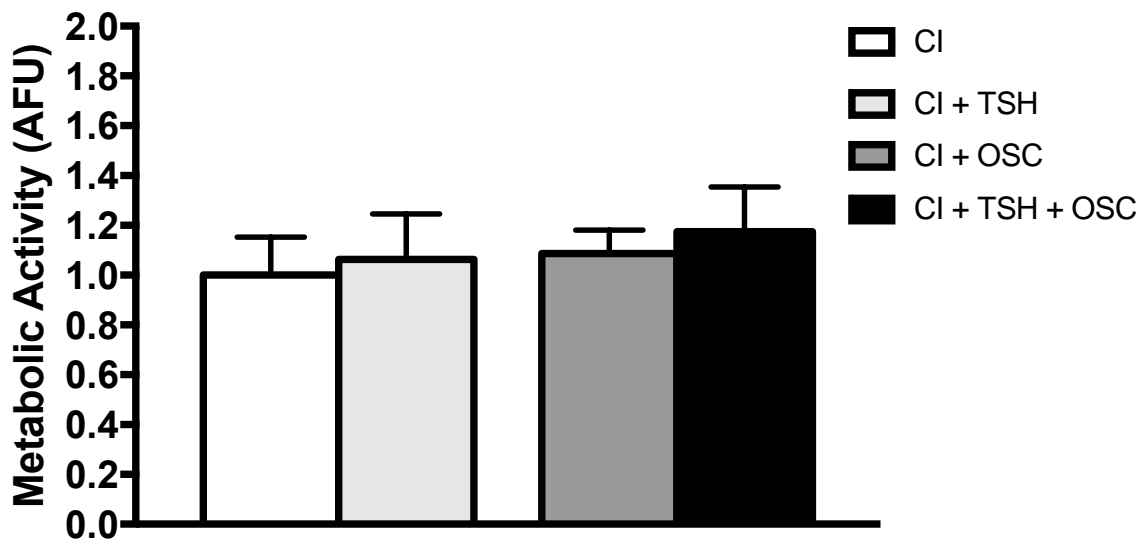


Figure 27. Metabolic activity of FRTL-5 cells cultured on adsorbed collagen type I.

There was no significance observed.

Metabolic activity was also measured on FRTL- cultured on BM (Figure 28). Exposure to oscillation increased their metabolic activity by $36.23\% \pm 18.8$ and inclusion of TSH increased their metabolic activity by $34.6\% \pm 10.2$. Incubation with TSH increased metabolic activity by $12.7\% \pm 9.2$.

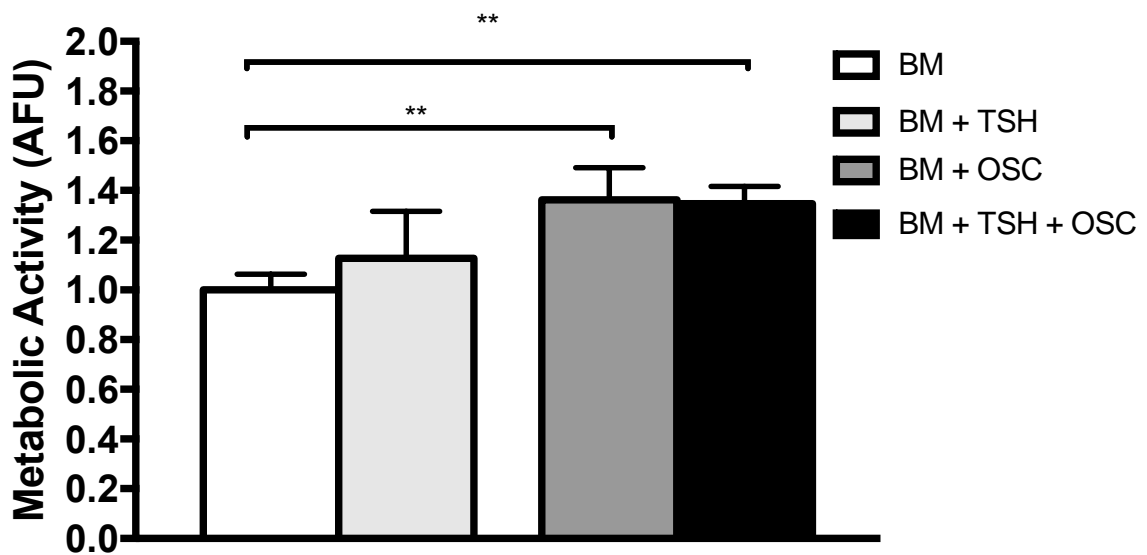
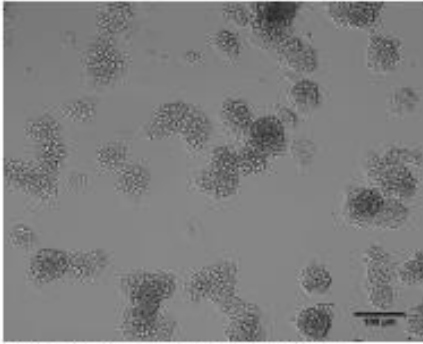


Figure 28. Metabolic activity of FRTL-5 cells cultured on basement membrane.

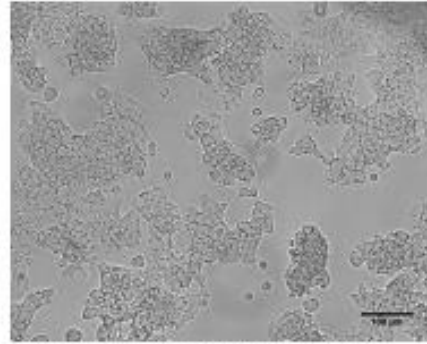
Oscillation and TSH plus oscillation had a significance increase over the control group ($p < 0.01$).

Cellular morphology was observed when FRTL-5 cells were cultured without TSH (Figure 29c). This image shows how the cell morphology is changed due to the lack to TSH stimulation. The FRTL-5 cells appear to have a larger structure without a very well defined cell membrane. When FRTL-5 cells are reintroduced to TSH at 1 mU/mL concentration for 24 hours, they appear to retake the same morphology as FRTL-5 cells with constant TSH exposure (Figure 29d). Exposure to acceleration without TSH stimulation appeared to have the same morphological response as TSH stimulation (Figure 29b).

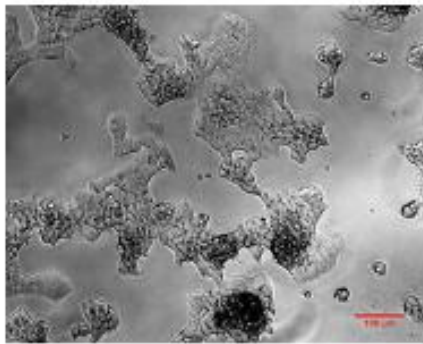
(A) FRTL-5 Cells Grown in 6H Media



(B) FRTL-5 OSC 1m/s^2 for 24 Hours



(C) TSH Deprivation for 4 Days



(D) OSC 1m/s^2 for 24 Hours in 6H

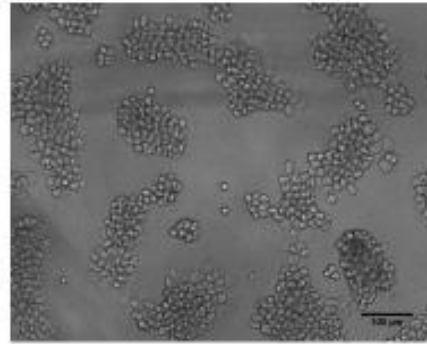


Figure 29. Effects of vibration on FRTL-5 morphology. FRTL-5 cells are culture in 6H media (1 mU/mL TSH) (A). This is the typical morphology normally associated with the culture of FRTL-5 cells. When FRTL-5 cells are deprived of TSH, they have a different morphology (B). FRTL-5 cells were then exposed to oscillation at 1m/s^2 for 24 hours (C). The morphology appears to have shifted back to more rounded shape similar to growth in 6H media. FRTL- 5 cells were also oscillated in 6H media (D). These cells show a similar morphology to group A.

Discussion and Conclusion

The importance of ECM for cellular function has been clearly stated (144, 146). Previous research in thyroid epithelial function has predominantly been conducted on tissue culture polystyrene. Our preliminary work in this chapter has highlighted some different cell behavior on ECM proteins as compared to TCPS. Firstly, a clear change in cell morphology is noticed. The goal of future work is to create a thyroid follicle, study follicle formation, and determine their response to mechanical stimulation. This goal of creating a follicle will eliminate one of the project limitations of experimenting of FRTL-5 cells in a monolayer on tissue culture polystyrene.

Another difference is noticed in the metabolic activity assay. When FRTL-5 cells are cultured on adsorbed collagen type I, their response to hormonal and mechanical stimulation are reduced when compared to TCPS. However, when FRTL-5 cells are stimulated on BM their metabolic activity is increased compared to their response on TCPS. This response may be because the BM is a gel with a softer stiffness. The collagen type I gel is adsorbed on the plastic, so FRTL-5 likely sense the same stiffness as TCPS. Also, epithelial are normally cultured on BM proteins as opposed to collagen type I.

The cytoskeleton structure is also an interesting topic. In chapter 3, I investigated the mechanosensing role of actin polymerization and the Rho/ROCK pathway in FRTL-5. I believe this area is open for further exploration. The thyroid epithelial response may be due to a change in the actin structure. In this chapter we have noticed FRTL-5 morphological differences in both of the cellular responses to hormonal and physical

stimulation. A better understanding of this mechanism may lead to greater opportunities and further uses of vibration to positively influence thyroid epithelial cells.

The substrates on which these cells are cultured is also of great importance. It has been shown that thyroid cancer can be directly related to thyroid tissue stiffness. It could be important to mimic this *in vivo* condition while conducting *in vitro* experiments. One potential way to accomplish this is to culture and expose thyroid epithelial cells to vibrations on more physiological substrates with varying stiffness. I have initially tried to create a gel of varying stiffness in a 96-well plate. This was done so it could be attached to the TRB. With the Voice Coil Bioreactor, we are not under the constraints to use the same wells as the TRB. This could allow us to study how vibrations affect individuals with varying thyroid conditions.

In conclusion, the initial work presented in this dissertation represents the first look at the mechanical stimulation of the thyroid tissue provided by stimulated vocalization. I have demonstrated that FRTL-5 cells produced key markers for thyroid hormone production in response to mechanical stimulation, and this response is dependent on oscillation dosage. I have also demonstrated that actin polymerization plays a role in FRTL-5 cells' ability to sense these mechanical stimuli. To further improve on this data, a 3-Dimensional environment should be created to better mimic the physiological state. A 3-D culture may also provide a better understanding of how thyroid epithelial cells respond to their mechanical surroundings.

Appendix: Protocols

Media Preparation

Bovine Calf Serum (BCS)

- 1) Aliquot 50 mL of stock solution and store at -20 degrees Celsius
- 2) Remove from freezer and let thaw at room temperature
- 3) Once thawed, place in 900 mL of distilled water

Ham's F-12 medium with Coon's modification (Sigma)

- 1) Store at 4 degrees Celsius
- 2) Remove one vial from fridge and mix with water and BCS

Transferrin- 100 mg

Final Concentration: 0.005 mg/mL in 1 L of media

- 1) Take stock powder and dissolve in 1 mL of distilled water
- 2) This gives a stock concentration of 0.1 mg/1 uL
- 3) Aliquot 50 uL of solution and store at -20 degrees Celsius
- 4) Thaw 1 of the 50 uL aliquot and mix with the media solution

Somastatin- 0.1 mg

Final concentration: 10 ng/mL in 1 L of media

- 1) Add 1 mL of distilled water to somastatin powder
- 2) Makes a concentration of 0.1 mg/mL
- 3) Aliquot 100 uL of stock solution and store at -20 degrees Celsius
- 4) Remove one vial and mix with media solution

Gly-his-lys acetate 0.5 mg

Final Concentration: 10 ng/ mL

- 1) Add 0.5 mL of water to gly-his-lys powder
- 2) Stock solution is now 1 ug/uL
- 3) Aliquot in 10 uL sizes
- 4) Thaw and mix one aliquot

Final concentration: 10 ng/mL in 1 L of media

Insulin- 1 mg/mL

Final concentration: 0.01 mg/mL in 1 L of media

Stock solution from Sigma is

TSH- 10 I.U.

Final concentration: 1 mU/mL in 1 L of media

- 1) Dissolve TSH in 2 mL of distilled water

- 2) Stock solution in 5 Units TSH/mL
- 3) Aliquot in 100 uL sizes and store at -20 degrees Celsius
- 4) Add in aliquot of 100 uL/ 500 mL of media
- 5) Final media concentration is 1 mU/mL of media

Hydrocortisone-

10 nM

Sodium Bicarbonate

- 1) Add 1.5 g of sodium bicarbonate

Add distilled water to a final volume of 1 Liter

Cyclic Adenosine Monophosphate (cAMP) Assay

- 1) Immediately following the vibration conditions, place 25 uL of 0.1M HCl into each well
- 2) Incubate the cells in 0.1 HCl at room temperature for 10 minutes
- 3) Inspect the cells under microscope to confirm cells have lysed
- 4) Centrifuge at 5000 rpm for 3 minutes
- 5) Freeze the supernatant at -80 degrees Celsius to be assayed later

Created cAMP standard curve

- 1) Allow the stock cAMP solution (2000 pmol/ml) to warm to room temperature
- 2) Add 5 mL of the supplied Wash Buffer Concentrate with 95 mL of deionized water
 - a. This is stable at room temperature for 3 months
- 3) Prepare the Assay with the acetylation reagents
 - a. This is needed because the small sample size and low concentration of cAMP
- 4) Add 0.5 mL of Acetic Acid Anhydride to 1 mL of Triethylamine
 - a. Use solution from step 3 within 60 minutes of mixing the two solutions
- 5) Create 5 different concentrations of cAMP standard
 - a. First, add 10 uL of stock solution to 990 uL of the 0.1 HCl for a 20 pmol/mL concentration
 - b. Serial dilute that sample by a quarter for a 5 pmol/mL concentration
 - c. Follow step 5.b for 3 more serial dilutions
 - d. This yield a concentration range of 20, 5, 1.25, 0.312, 0.078 pmol/mL
- 6) Add 10 uL of acetylating reagent for each 200 uL of standard sample
 - a. Acetylated standard should be used within 30 minutes

Assay Protocol

- 1) Pipet 50 uL of neutralizing Reagent into each well of the treated 96 well plate except the total activity and Blank wells
- 2) Pipet 100 uL of the 0.1 HCL into the non-specific binding and Bo wells
- 3) Pipet 50 uL of 0.1 HCl to the NSB well
- 4) Pipet 100 uL of standards 1 through 5 into the marked wells
- 5) Pipet 100 uL of the samples in to the marked wells
- 6) Pipet 50 uL of the blue conjugate into each well except the TA and blank wells
- 7) Pipet 50 uL of the yellow antibody into each well except the TA, blank, and NSB wells
- 8) Seal plate and incubate for 2 hours at room temperature on a plate shaker set to 500 rpm
- 9) Remove all liquid from each well
- 10) Wash with 400 uL of washing buffer 3 times
- 11) Pipet 5 uL of the blue conjugate to the TA wells
- 12) Add 200 uL of substrate into each well
- 13) Incubate for 1 hour at room temperature
- 14) Pipet 50 uL of stop solution into each well
- 15) Read optical density at 405 nm
- 16) Subtract the mean optical density of the substrate blank from all readings

DCF Protocol (Reactive Oxygen Detection)

- 1) Dilute dichlorofluorescein from thermos fischer
- 2) Immediately following an excitation protocol, remove all media from all wells.
- 3) Place 50 μ L of 10 μ M DCF in PBS solution into each well
- 4) Incubate at 37 °C for 30 minutes
- 5) Measure in fluorometer at Ex/EM = 495/520

Live Dead Protocol

Live Dead Stain (Molecular Probes L3224)

The Stock solutions with the kit are:

Ethidium homodimer (EthD-1): 2mM

Calcein AM CAM: 4mM

Store at -20 degees Celsius

- 1) Prepare the working solution of EthD-1 and CAM 1 hour before you will need it. The working solution is only good for the day it is made. Protect the solution from light.
- 2) Add 20 uL of EthD-1 to 10 mL of PBS
- 3) Add 5 uL of CAM to the same solution from above
 - a. Working concentration is 4 uM EthD-1 and 2 uM CAM
- 4) Add 100 uL of working solution into each well you want to analyze

- 5) Incubate at room temperature for 30 minutes

Multiwell Disc and TRB Setup

- 1) Turn on TRB heat source (It is set to 37 degrees Celsius) 30 minutes prior to starting
- 2) Turn on the computer attached to the rheometer
- 3) Start the bohlin software on the desktop
- 4) Prepare the appropriate amount of 10 mU/mL TSH F-12 media
 - a. 3.5 mL of the TSH media and TSH free media is needed per multiwell disc and control
 - b. Amount of TSH to be added

amount of stock TSH solution in mL

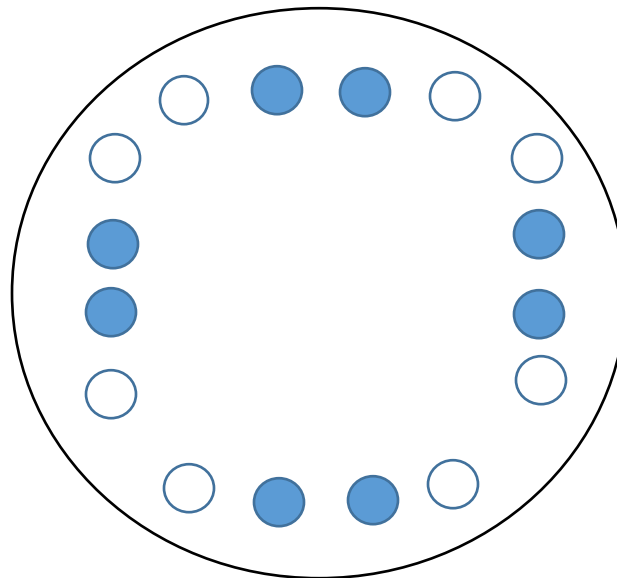
$$= \frac{(\text{number of disc} \times 3.5 \text{ mL}) \times 10 \frac{\text{mU}}{\text{mL}}}{2000 \text{ mU/mL}}$$

NOTE: this will be enough for the disc and controls

- 5) Add inhibitors to the media at this point if needed
- 6) Warm the media to 37 degrees Celsius
- 7) Remove the media from the disc and controls
- 8) Add the appropriate media to the wells

Column 1	Column 2
NO TSH	TSH

- 9) Fill the highlighted wells with media and make sure to label which well has which additives (e.g. TSH, Y27632)



- 10) Attach the disc to the parallel plate and acrylic base. Make sure the lid does NOT move when attached.
- 11) Attach the disc/parallel plate to the rheometer motor
- 12) Unlock the motor (make sure you have been trained or look at the rheometer manual)
- 13) In the bohrin software, click on the oscillation setting
- 14) Click on the gap tab
- 15) Hit zero. This will start to move the motor and disc till they touch the bottom plate.
- 16) After the rheometer has a set of steady zeros, move the stage up high enough to place double sided tape between the base and acrylic base attached to the disc
- 17) Lower the motor with parallel plate slowly until it is firmly attached to the double sided tape
- 18) Close out of the gap setting in the bohrin software
- 19) Set the correct vibration paramaters
 - a. Frequency
 - b. Strain
 - c. Duty cycle
 - d. Number of samples (this is for the time. Make sure it is long enough for your desired time)
 - e. Set a separate timer for your desired time
- 20) Strain calculation

$$strain = \frac{acceleration}{angular\ frequency \times gap}$$

Rheometer setting for frequency is cycles not angular

Gap is in millimeters

- 21) Press start and make sure the graph in the software has two sinusoidal waves

REFERENCES

1. Albi E, Curcio F, Lazzarini A, Floridi A, Cataldi S, Lazzarini R, et al. A firmer understanding of the effect of hypergravity on thyroid tissue: cholesterol and thyrotropin receptor. *PloS one*. 2014;9(5):e98250.
2. Ma X, Wehland M, Aleshcheva G, Hauslage J, Wasser K, Hemmersbach R, et al. Interleukin-6 Expression under Gravitational Stress Due to Vibration and Hypergravity in Follicular Thyroid Cancer Cells. *Plos One*. 2013;8(7).
3. Popolo PS. Relating Vocal Fold Vibration Amplitude To Skin Acceleration Level on the Anterior Neck. University of Iowa. 2007;Graduate Thesis.
4. Kimura T, Okajima F, Sho K, Kobayashi I, Kondo Y. Thyrotropin-Induced Hydrogen-Peroxide Production in FRTL-5 Thyroid-Cells Is Mediated Not by Adenosine-3',5'-Monophosphate, but by Ca²⁺ Signaling Followed by Phospholipase-A2 Activation and Potentiated by an Adenosine Derivative. *Endocrinology*. 1995;136(1):116-23.
5. Allgeier A, Offermanns S, Van Sande J, Spicher K, Schultz G, Dumont JE. The human thyrotropin receptor activates G-proteins Gs and Gq/11. *The Journal of biological chemistry*. 1994;269(19):13733-5.
6. Ahad F, Ganie SA. Iodine, Iodine metabolism and Iodine deficiency disorders revisited. *Indian J Endocrinol Metab*. 2010;14(1):13-7.
7. Bizhanova A, Kopp P. Minireview: The Sodium-Iodide Symporter NIS and Pendrin in Iodide Homeostasis of the Thyroid. *Endocrinology*. 2009;150(3):1084-90.
8. Song Y, Driessens N, Costa M, De Deken X, Detours V, Corvilain B, et al. Roles of hydrogen peroxide in thyroid physiology and disease. *J Clin Endocrinol Metab*. 2007;92(10):3764-73.
9. Häggström M. Medical gallery of Mikael Häggström *WikiJournal of Medicine*. 2014;1(2).
10. Braverman LE, Ingbar SH, Sterling K. Conversion of thyroxine (T4) to triiodothyronine (T3) in athyreotic human subjects. *J Clin Invest*. 1970;49(5):855-64.
11. Hasselstrom K, Siersbaek-Nielsen K, Lumholtz IB, Faber J, Kirkegaard C, Friis T. The bioavailability of thyroxine and 3,5,3'-triiodothyronine in normal subjects and in hyper- and hypothyroid patients. *Acta Endocrinol (Copenh)*. 1985;110(4):483-6.
12. Ingbar SH, Braverman LE. Active form of the thyroid hormone. *Annu Rev Med*. 1975;26:443-9.
13. Siegel RL, Miller KD, Jemal A. Cancer statistics, 2016. *CA Cancer J Clin*. 2016;66(1):7-30.
14. Krohn K, Maier J, Paschke R. Mechanisms of disease: hydrogen peroxide, DNA damage and mutagenesis in the development of thyroid tumors. *Nature clinical practice Endocrinology & metabolism*. 2007;3(10):713-20.
15. Ohye H, Sugawara M. Dual oxidase, hydrogen peroxide and thyroid diseases. *Experimental biology and medicine*. 2010;235(4):424-33.
16. Kim H, Lee TH, Park ES, Suh JM, Park SJ, Chung HK, et al. Role of peroxiredoxins in regulating intracellular hydrogen peroxide and hydrogen peroxide-induced apoptosis in thyroid cells. *The Journal of biological chemistry*. 2000;275(24):18266-70.
17. Mutaku JF, Poma JF, Many MC, Deneff JF, van den Hove MF. Cell necrosis and apoptosis are differentially regulated during goitre development and iodine-induced involution. *J Endocrinol*. 2002;172(2):375-86.
18. Maier J, van Steeg H, van Oostrom C, Paschke R, Weiss RE, Krohn K. Iodine deficiency activates antioxidant genes and causes DNA damage in the thyroid gland of rats and mice. *Biochimica et biophysica acta*. 2007;1773(6):990-9.

19. Avbelj M, Tahirovic H, Debeljak M, Kusekova M, Toromanovic A, Krzisnik C, et al. High prevalence of thyroid peroxidase gene mutations in patients with thyroid dysmorphogenesis. *European journal of endocrinology / European Federation of Endocrine Societies.* 2007;156(5):511-9.
20. Hashemipour M, Soheilipour F, Karimizare S, Khanahmad H, Karimipour M, Aminzadeh S, et al. Thyroid peroxidase gene mutation in patients with congenital hypothyroidism in isfahan, iran. *International journal of endocrinology.* 2012;2012:717283.
21. Canaris GJ, Manowitz NR, Mayor G, Ridgway EC. The Colorado thyroid disease prevalence study. *Arch Intern Med.* 2000;160(4):526-34.
22. Chakera AJ, Pearce SH, Vaidya B. Treatment for primary hypothyroidism: current approaches and future possibilities. *Drug Des Devel Ther.* 2012;6:1-11.
23. Asvold BO, Bjoro T, Platou C, Vatten LJ. Thyroid function and the risk of coronary heart disease: 12-year follow-up of the HUNT study in Norway. *Clinical endocrinology.* 2012;77(6):911-7.
24. Tarraga Lopez PJ, Lopez CF, de Mora FN, Montes JA, Alberio JS, Manez AN, et al. Osteoporosis in patients with subclinical hypothyroidism treated with thyroid hormone. *Clinical cases in mineral and bone metabolism : the official journal of the Italian Society of Osteoporosis, Mineral Metabolism, and Skeletal Diseases.* 2011;8(3):44-8.
25. Fuller-Thomson E, Saini J, Brennenstuhl S. The association between depression and thyroid disorders in a regionally representative Canadian sample. *Psychol Health Med.* 2012;17(3):335-45.
26. Elder J MA, O'Reilly DS, Packard CJ, Series JJ, Shepherd, Jabbar A. The relationship between serum cholesterol and serum thyrotropin, thyroxine and tri-iodothyronine concentrations in suspected hypothyroidism. *Ann Clin Biochem.* 1990;27:110-3.
27. Kantor ED, Rehm CD, Haas JS, Chan AT, Giovannucci EL. Trends in Prescription Drug Use Among Adults in the United States From 1999-2012. *Obstetrical & Gynecological Survey.* 2016;71(3):131-3.
28. Okosieme OE, Belludi G, Spittle K, Kadiyala R, Richards J. Adequacy of thyroid hormone replacement in a general population. *QJM : monthly journal of the Association of Physicians.* 2011;104(5):395-401.
29. Whalley PD. Do abnormal thyroid stimulating hormone level values result in treatment changes? A study of patients on thyroxine in one general practice. *British Journal of General Practice.* 1995;45:93-5.
30. Mazokopakis EE, Giannakopoulos TG, Starakis IK. Interaction between levothyroxine and calcium carbonate. *Can Fam Physician.* 2008;54(1):39-.
31. Bach-Huynh TG, Nayak B, Loh J, Soldin S, Jonklaas J. Timing of levothyroxine administration affects serum thyrotropin concentration. *The Journal of clinical endocrinology and metabolism.* 2009;94(10):3905-12.
32. Bolk N, Visser TJ, Nijman J, Jongste IJ, Tijssen JG, Berghout A. Effects of evening vs morning levothyroxine intake: a randomized double-blind crossover trial. *Archives of internal medicine.* 2010;170(22):1996-2003.
33. Rajput R, Chatterjee S, Rajput M. Can Levothyroxine Be Taken as Evening Dose? Comparative Evaluation of Morning versus Evening Dose of Levothyroxine in Treatment of Hypothyroidism. *Journal of thyroid research.* 2011;2011:505239.
34. Vaidya B, Pearce SH. Management of hypothyroidism in adults. *BMJ.* 2008;337:a801.
35. Cooper DS. Clinical practice. Subclinical hypothyroidism. *N Engl J Med.* 2001;345(4):260-5.
36. Vandenburg H, Chromiak J, Shansky J, Del Tatto M, Lemaire J. Space travel directly induces skeletal muscle atrophy. *FASEB J.* 1999;13(9):1031-8.
37. White RJ, Averner M. Humans in space. *Nature.* 2001;409(6823):1115-8.

38. Masini MA, Albi E, Barmo C, Bonfiglio T, Bruni L, Canesi L, et al. The impact of long-term exposure to space environment on adult mammalian organisms: a study on mouse thyroid and testis. *PloS one*. 2012;7(4):e35418.
39. Meli A, Perrella G, Curcio F, Ambesi-Impiombato FS. Response to hypogravity of normal in vitro cultured follicular cells from thyroid. *Acta astronautica*. 1998;42(1-8):465-72.
40. Leary CJ, Harris S. Steroid hormone levels in calling males and males practicing alternative non-calling mating tactics in the green treefrog, *Hyla cinerea*. *Hormones and behavior*. 2013;63(1):20-4.
41. Riters LV. The role of motivation and reward neural systems in vocal communication in songbirds. *Frontiers in neuroendocrinology*. 2012;33(2):194-209.
42. Catchpole CK, Slater PJB. *Bird Song Biological Themes and Variations* Second Edition Introduction. *Bird Song: Biological Themes and Variations*, 2nd Edition. 2008:ix-+.
43. Svec JG, Titze IR, Popolo PS. Estimation of sound pressure levels of voiced speech from skin vibration of the neck. *J Acoust Soc Am*. 2005;117(3 Pt 1):1386-94.
44. Abercromby AF, Amonette WE, Layne CS, McFarlin BK, Hinman MR, Paloski WH. Vibration exposure and biodynamic responses during whole-body vibration training. *Med Sci Sports Exerc*. 2007;39(10):1794-800.
45. Barr DA, Kernohan WG, Mollan RA. Transient vibrations caused by heel strike. *Proc Inst Mech Eng H*. 1990;204(2):135-7.
46. Beck BR. Vibration Therapy to Prevent Bone Loss and Falls: Mechanisms and Efficacy. *Curr Osteoporos Rep*. 2015;13(6):381-9.
47. Bosco C, Iacovelli M, Tsarpela O, Cardinale M, Bonifazi M, Tihanyi J, et al. Hormonal responses to whole-body vibration in men. *European journal of applied physiology*. 2000;81(6):449-54.
48. Heaver C, Goonetilleke KS, Ferguson H, Shiralkar S. Hand-arm vibration syndrome: a common occupational hazard in industrialized countries. *The Journal of hand surgery, European volume*. 2011;36(5):354-63.
49. Riihimaki H, Viikarijuntura E, Moneta G, Kuha J, Videman T, Tola S. Incidence of Sciatic Pain among Men in Machine Operating, Dynamic Physical Work, and Sedentary Work - a 3-Year Follow-Up. *Spine*. 1994;19(2):138-42.
50. Rolke R, Rolke S, Vogt T, Birklein F, Geber C, Treede RD, et al. Hand-arm vibration syndrome: clinical characteristics, conventional electrophysiology and quantitative sensory testing. *Clin Neurophysiol*. 2013;124(8):1680-8.
51. Zeeman ME, Kartha S, Winkelstein BA. Whole-Body Vibration Induces Pain and Lumbar Spinal Inflammation Responses in the Rat That Vary With the Vibration Profile. *Journal of Orthopaedic Research*. 2016;34(8):1439-46.
52. Zeeman ME, Kartha S, Jaumard NV, Baig HA, Stablow AM, Lee J, et al. Whole-body Vibration at Thoracic Resonance Induces Sustained Pain and Widespread Cervical Neuroinflammation in the Rat. *Clinical Orthopaedics and Related Research*. 2015;473(9):2936-47.
53. Hulshof C, van Zanten BV. Whole-body vibration and low-back pain. A review of epidemiologic studies. *Int Arch Occup Environ Health*. 1987;59(3):205-20.
54. Cardinale M, Leiper J, Erskine J, Milroy M, Bell S. The acute effects of different whole body vibration amplitudes on the endocrine system of young healthy men: a preliminary study. *Clinical physiology and functional imaging*. 2006;26(6):380-4.
55. Di Loreto C, Ranchelli A, Lucidi P, Murdolo G, Parlanti N, De Cicco A, et al. Effects of whole-body vibration exercise on the endocrine system of healthy men. *Journal of endocrinological investigation*. 2004;27(4):323-7.
56. Couto BP, Silva HR, Filho AG, da Silveira Neves SR, Ramos MG, Szmuchrowski LA, et al. Acute Effects of Resistance Training with Local Vibration. *International journal of sports medicine*. 2013.

57. Kalyani BG, Venkatasubramanian G, Arasappa R, Rao NP, Kalmady SV, Behere RV, et al. Neurohemodynamic correlates of 'OM' chanting: A pilot functional magnetic resonance imaging study. *International journal of yoga*. 2011;4(1):3-6.
58. Jindrak KF, Jindrak H. Mechanical effect of vocalization on human brain and meninges. *Medical hypotheses*. 1988;25(1):17-20.
59. Wu XT, Sun LW, Qi HY, Shi H, Fan YB. The bio-response of osteocytes and its regulation on osteoblasts under vibration. *Cell Biol Int*. 2016;40(4):397-406.
60. Uzer G, Pongkitwitoon S, Ian C, Thompson WR, Rubin J, Chan ME, et al. Gap junctional communication in osteocytes is amplified by low intensity vibrations in vitro. *PLoS One*. 2014;9(3):e90840.
61. Uzer G, Thompson WR, Sen B, Xie Z, Yen SS, Miller S, et al. Cell Mechanosensitivity to Extremely Low-Magnitude Signals Is Enabled by a LINCed Nucleus. *Stem Cells*. 2015;33(6):2063-76.
62. Fortemaision N, Blancquaert S, Dumont JE, Maenhaut C, Aktories K, Roger PP, et al. Differential involvement of the actin cytoskeleton in differentiation and mitogenesis of thyroid cells: inactivation of Rho proteins contributes to cyclic adenosine monophosphate-dependent gene expression but prevents mitogenesis. *Endocrinology*. 2005;146(12):5485-95.
63. Ikeda K, Ishizuka H, Sawada A, Urushiyama K. Vibration acceleration magnitudes of hand-held tools and workpieces. *Ind Health*. 1998;36(2):197-208.
64. Titze IR, Svec JG, Popolo PS. Vocal dose measures: quantifying accumulated vibration exposure in vocal fold tissues. *J Speech Lang Hear Res*. 2003;46(4):919-32.
65. Ozcivici E, Luu YK, Rubin CT, Judex S. Low-level vibrations retain bone marrow's osteogenic potential and augment recovery of trabecular bone during reambulation. *PLoS One*. 2010;5(6):e11178.
66. McCann MR, Patel P, Pest MA, Ratneswaran A, Lalli G, Beaucage KL, et al. Repeated exposure to high-frequency low-amplitude vibration induces degeneration of murine intervertebral discs and knee joints. *Arthritis Rheumatol*. 2015;67(8):2164-75.
67. Heaver B, Hutton SB. Keeping an eye on the truth? Pupil size changes associated with recognition memory. *Memory*. 2011;19(4):398-405.
68. Hughes JM, Wirth O, Krajnak K, Miller R, Flavahan S, Berkowitz DE, et al. Increased oxidant activity mediates vascular dysfunction in vibration injury. *The Journal of pharmacology and experimental therapeutics*. 2009;328(1):223-30.
69. White CR, Haidekker MA, Stevens HY, Frangos JA. Extracellular signal-regulated kinase activation and endothelin-1 production in human endothelial cells exposed to vibration. *J Physiol*. 2004;555(Pt 2):565-72.
70. Krajnak K, Dong RG, Flavahan S, Welcome D, Flavahan NA. Acute vibration increases alpha2C-adrenergic smooth muscle constriction and alters thermosensitivity of cutaneous arteries. *J Appl Physiol (1985)*. 2006;100(4):1230-7.
71. Couto BP, Silva HR, Filho AG, da Silveira Neves SR, Ramos MG, Szmuchrowski LA, et al. Acute effects of resistance training with local vibration. *International journal of sports medicine*. 2013;34(9):814-9.
72. Vanderpump MP. The epidemiology of thyroid disease. *Br Med Bull*. 2011;99:39-51.
73. Barrett EJ. The Thyroid Gland. In: Boron WFB, E.L., editor. *Medical Physiology: A Cellular And Molecular Approach*; Elsevier; 2012. p. 1044-56.
74. Meli A, Perrella G, Curcio F, Ambesi-Impiombato FS. Response to hypogravity of normal in vitro cultured follicular cells from thyroid. *Acta Astronaut*. 1998;42(1-8):465-72.
75. Chen AY, Jemal A, Ward EM. Increasing incidence of differentiated thyroid cancer in the United States, 1988-2005. *Cancer*. 2009;115(16):3801-7.
76. Klemuk SA, Vigmostad S, Endapally K, Wagner AP, Titze IR. A multiwell disc appliance used to deliver quantifiable accelerations and shear stresses at sonic frequencies. *Processes*. 2014;2(1):71-88.

77. Klemuk SA, Jaiswal S, Titze IR. Cell viability viscoelastic measurement in a rheometer used to stress and engineer tissues at low sonic frequencies. *The Journal of the Acoustical Society of America*. 2008;124(4):2330-9.
78. Titze IR, Klemuk SA, Gray S. Methodology for rheological testing of engineered biomaterials at low audio frequencies. *The Journal of the Acoustical Society of America*. 2004;115(1):392-401.
79. Ambesi-Impiombato FS. Living, fast-growing thyroid cell strain, FRTL-5. Google Patents; 1986.
80. Kohn LD, Valente WA, Grollman-Wolff EF, Aloj SM, Vitti P. Clinical determination and/or quantification of thyrotropin and a variety of thyroid stimulatory or inhibitory factors performed in vitro with an improved thyroid cell line, FRTL-5. Google Patents; 1986.
81. Bidey S, Chiovato L, Day A, Turmaine M, Gould R, Ekins R, et al. Evaluation of the rat thyroid cell strain FRTL-5 as an in-vitro bioassay system for thyrotrophin. *Journal of endocrinology*. 1984;101(3):269-NP.
82. Lorenz S, Eszlinger M, Paschke R, Aust G, Weick M, Führer D, et al. Calcium signaling of thyrocytes is modulated by TSH through calcium binding protein expression. *Biochimica et Biophysica Acta (BBA)-Molecular Cell Research*. 2010;1803(3):352-60.
83. Vainio M, Fredholm BB, Törnquist K. Thyrotropin regulates adenosine A1 receptor expression in rat thyroid FRTL-5 cells. *British journal of pharmacology*. 2000;130(2):471-7.
84. Ambesi-Impiombato FS, Villone G. The FRTL-5 thyroid cell strain as a model for studies on thyroid cell growth. *Acta Endocrinologica*. 1987;116(1 Suppl):S242-S5.
85. Björkman U, Ekholm R. Hydrogen peroxide generation and its regulation in FRTL-5 and porcine thyroid cells. *Endocrinology*. 1992;130(1):393-9.
86. Li X, Lu S, Miyagi E, Katoh R, Kawaoi A. Thyrotropin prevents apoptosis by promoting cell adhesion and cell cycle progression in FRTL-5 cells. *Endocrinology*. 1999;140(12):5962-70.
87. Titze IR, Hunter EJ, Švec JG. Voicing and silence periods in daily and weekly vocalizations of teachers. *The Journal of the Acoustical Society of America*. 2007;121(1):469-78.
88. Popolo PS. Relating Vocal Fold Vibration Amplitude To Skin Acceleration Level on the Anterior Neck: Univeristy of Iowa; 2007.
89. Gloeckner H, Jonuleit T, Lemke HD. Monitoring of cell viability and cell growth in a hollow-fiber bioreactor by use of the dye Alamar Blue. *Journal of immunological methods*. 2001;252(1-2):131-8.
90. Wang H, Joseph JA. Quantifying cellular oxidative stress by dichlorofluorescein assay using microplate reader. *Free Radical Biology and Medicine*. 1999;27(5):612-6.
91. Rivas M, Santisteban P. TSH-activated signaling pathways in thyroid tumorigenesis. *Molecular and cellular endocrinology*. 2003;213(1):31-45.
92. Santisteban P, Kohn L, Di Lauro R. Thyroglobulin gene expression is regulated by insulin and insulin-like growth factor I, as well as thyrotropin, in FRTL-5 thyroid cells. *Journal of Biological Chemistry*. 1987;262(9):4048-52.
93. Spitzweg C, Joba W, Morris J, Heufelder A. Regulation of sodium iodide symporter gene expression in FRTL-5 rat thyroid cells. *Thyroid*. 1999;9(8):821-30.
94. Kimura T, Okajima F, Sho K, Kobayashi I, Kondo Y. Thyrotropin-induced hydrogen peroxide production in FRTL-5 thyroid cells is mediated not by adenosine 3', 5'-monophosphate, but by Ca²⁺ signaling followed by phospholipase-A2 activation and potentiated by an adenosine derivative. *Endocrinology*. 1995;136(1):116-23.
95. Pomerance M, Abdullah HB, Kamerji S, Correze C, Blondeau JP. Thyroid-stimulating hormone and cyclic AMP activate p38 mitogen-activated protein kinase cascade. Involvement of protein kinase A, rac1, and reactive oxygen species. *J Biol Chem*. 2000;275(51):40539-46.
96. Syedain ZH, Weinberg JS, Tranquillo RT. Cyclic distension of fibrin-based tissue constructs: evidence of adaptation during growth of engineered connective tissue. *Proceedings of the National Academy of Sciences of the United States of America*. 2008;105(18):6537-42.

97. Thompson WR, Yen SS, Rubin J. Vibration therapy: clinical applications in bone. *Current opinion in endocrinology, diabetes, and obesity*. 2014;21(6):447.
98. Chan ME, Uzer G, Rubin CT. The potential benefits and inherent risks of vibration as a non-drug therapy for the prevention and treatment of osteoporosis. *Current osteoporosis reports*. 2013;11(1):36-44.
99. Garman R, Gaudette G, Donahue LR, Rubin C, Judex S. Low-level accelerations applied in the absence of weight bearing can enhance trabecular bone formation. *Journal of Orthopaedic Research*. 2007;25(6):732-40.
100. Castillo AB, Alam I, Tanaka SM, Levenda J, Li J, Warden SJ, et al. Low-amplitude, broad-frequency vibration effects on cortical bone formation in mice. *Bone*. 2006;39(5):1087-96.
101. Rubin C, Capilla E, Luu Y, Busa B, Crawford H, Nolan D, et al. Adipogenesis is inhibited by brief, daily exposure to high-frequency, extremely low-magnitude mechanical signals. *Proceedings of the National Academy of Sciences*. 2007;104(45):17879-84.
102. Thompson WR, Keller BV, Davis ML, Dahners LE, Weinhold PS. Low-Magnitude, High-Frequency Vibration Fails to Accelerate Ligament Healing but Stimulates Collagen Synthesis in the Achilles Tendon. *Orthopaedic journal of sports medicine*. 2015;3(5):2325967115585783.
103. Rosenberg N, Levy M, Francis M. Experimental model for stimulation of cultured human osteoblast-like cells by high frequency vibration. *Cytotechnology*. 2002;39(3):125-30.
104. Jing D, Tong S, Zhai M, Li X, Cai J, Wu Y, et al. Effect of low-level mechanical vibration on osteogenesis and osseointegration of porous titanium implants in the repair of long bone defects. *Sci Rep*. 2015;5:17134.
105. Pongkitwitoon S, Weinheimer-Haus EM, Koh TJ, Judex S. Low-intensity vibrations accelerate proliferation and alter macrophage phenotype in vitro. *Journal of biomechanics*. 2016.
106. Versaevel M, Braquenier J-B, Riaz M, Grevesse T, Lantoine J, Gabriele S. Super-resolution microscopy reveals LINC complex recruitment at nuclear indentation sites. *Scientific reports*. 2014;4.
107. Iyer KV, Pulford S, Mogilner A, Shivashankar G. Mechanical activation of cells induces chromatin remodeling preceding MKL nuclear transport. *Biophysical journal*. 2012;103(7):1416-28.
108. Wang N, Tytell JD, Ingber DE. Mechanotransduction at a distance: mechanically coupling the extracellular matrix with the nucleus. *Nature reviews Molecular cell biology*. 2009;10(1):75-82.
109. Guilluy C, Osborne LD, Van Landeghem L, Sharek L, Superfine R, Garcia-Mata R, et al. Isolated nuclei adapt to force and reveal a mechanotransduction pathway within the nucleus. *Nature cell biology*. 2014;16(4):376.
110. Klemuk Sea. A Multiwell Disc Appliance Used to Deliver Quantifiable Accelerations and Shear Stresses at Soinic Frequencies. *Proesses*. 2014;2(1):71-88.
111. Wu XT, Sun LW, Qi HY, Shi H, Fan YB. The bio-response of osteocytes and its regulation on osteoblasts under vibration. *Cell biology international*. 2016.
112. Coughlin TR, Niebur GL. Fluid shear stress in trabecular bone marrow due to low-magnitude high-frequency vibration. *Journal of biomechanics*. 2012;45(13):2222-9.
113. Kimura T, Van Keymeulen A, Golstein J, Fusco A, Dumont JE, Roger PP. Regulation of thyroid cell proliferation by TSH and other factors: a critical evaluation of in vitro models. *Endocrine reviews*. 2001;22(5):631-56.
114. Toda S, Aoki S, Uchihashi K, Matsunobu A, Yamamoto M, Ootani A, et al. Culture models for studying thyroid biology and disorders. *ISRN endocrinology*. 2011;2011.
115. Engler AJ, Sen S, Sweeney HL, Discher DE. Matrix elasticity directs stem cell lineage specification. *Cell*. 2006;126(4):677-89.
116. Zarkoob H, Bodduluri S, Ponnaluri SV, Selby JC, Sander EA. Substrate Stiffness Affects Human Keratinocyte Colony Formation. *Cellular and molecular bioengineering*. 2015;8(1):32-50.

117. Evans ND, Minelli C, Gentleman E, LaPointe V, Patankar SN, Kallivretaki M, et al. Substrate stiffness affects early differentiation events in embryonic stem cells. *European cells & materials*. 2009;18:1-13; discussion -4.
118. Doyle AD, Wang FW, Matsumoto K, Yamada KM. One-dimensional topography underlies three-dimensional fibrillar cell migration. *The Journal of cell biology*. 2009;184(4):481-90.
119. Yamashita K, Fujita H, Kitajima K, Nishii Y. Inter- and intracellular luminal formation in porcine thyroid tissues cultured in a collagen substrate. *Arch Histol Cytol*. 1989;52(2):109-14.
120. Espanet H, Alquier C, Mauchamp J. Polarity reversal of inside-out thyroid follicles cultured on the surface of a reconstituted basement membrane matrix. *Exp Cell Res*. 1992;200(2):473-80.
121. De Jesus AM, Aghvami M, Sander EA. A Combined In Vitro Imaging and Multi-scale Modeling System for Studying the Role of Cell Matrix Interactions in Cutaneous Wound Healing *PloS one*. 2016(10.1371/journal.pone.0148254).
122. Neidlinger-Wilke C, Wilke HJ, Claes L. Cyclic stretching of human osteoblasts affects proliferation and metabolism: a new experimental method and its application. *J Orthop Res*. 1994;12(1):70-8.
123. Worton LE, Kwon RY, Gardiner EM, Gross TS, Srinivasan S. Enhancement of Flow-Induced AP-1 Gene Expression by Cyclosporin A Requires NFAT-Independent Signaling in Bone Cells. *Cell Mol Bioeng*. 2014;7(2):254-65.
124. Rosenberg N, Levy M, Francis M. Experimental model for stimulation of cultured human osteoblast-like cells by high frequency vibration. *Cytotechnology*. 2002;39(3):125-30.
125. A.P. Wagner SC, I.R. Titze, E.A. Sander. Vibratory stimulation enhances thyroid epithelial cell function. *Biochemistry and Biophysics Reports*. 2016;8:376-81.
126. Mitra SK, Hanson DA, Schlaepfer DD. Focal adhesion kinase: in command and control of cell motility. *Nat Rev Mol Cell Biol*. 2005;6(1):56-68.
127. Wolfenson H, Henis YI, Geiger B, Bershadsky AD. The heel and toe of the cell's foot: a multifaceted approach for understanding the structure and dynamics of focal adhesions. *Cell Motil Cytoskeleton*. 2009;66(11):1017-29.
128. Sharp WW, Simpson DG, Borg TK, Samarel AM, Terracio L. Mechanical forces regulate focal adhesion and costamere assembly in cardiac myocytes. *Am J Physiol*. 1997;273(2 Pt 2):H546-56.
129. Samarel AM. Costameres, focal adhesions, and cardiomyocyte mechanotransduction. *Am J Physiol Heart Circ Physiol*. 2005;289(6):H2291-301.
130. Wozniak MA, Desai R, Solski PA, Der CJ, Keely PJ. ROCK-generated contractility regulates breast epithelial cell differentiation in response to the physical properties of a three-dimensional collagen matrix. *J Cell Biol*. 2003;163(3):583-95.
131. Provenzano PP, Keely PJ. Mechanical signaling through the cytoskeleton regulates cell proliferation by coordinated focal adhesion and Rho GTPase signaling. *Journal of Cell Science*. 2011;124(8):1195-205.
132. Hirata H, Tatsumi H, Sokabe M. Mechanical forces facilitate actin polymerization at focal adhesions in a zyxin-dependent manner. *Journal of Cell Science*. 2008;121(17):2795-804.
133. Ghosh M, Song X, Mouneimne G, Sidani M, Lawrence DS, Condeelis JS. Cofilin promotes actin polymerization and defines the direction of cell motility. *Science*. 2004;304(5671):743-6.
134. Brown D, Stow JL. Protein trafficking and polarity in kidney epithelium: from cell biology to physiology. *Physiol Rev*. 1996;76(1):245-97.
135. Ishizaki T, Uehata M, Tamechika I, Keel J, Nonomura K, Maekawa M, et al. Pharmacological properties of Y-27632, a specific inhibitor of rho-associated kinases. *Mol Pharmacol*. 2000;57(5):976-83.

136. Goddette DW, Frieden C. Actin polymerization. The mechanism of action of cytochalasin D. *The Journal of biological chemistry*. 1986;261(34):15974-80.
137. Ho CL, Mou TY, Chiang PS, Weng CL, Chow NH. Mini chamber system for long-term maintenance and observation of cultured cells. *Biotechniques*. 2005;38(2):267-73.
138. Lythgo N, Eser P, de Groot P, Galea M. Whole-body vibration dosage alters leg blood flow. *Clin Physiol Funct Imaging*. 2009;29(1):53-9.
139. Bovenzi M. Hand-arm vibration syndrome and dose-response relation for vibration induced white finger among quarry drillers and stoneworkers. Italian Study Group on Physical Hazards in the Stone Industry. *Occup Environ Med*. 1994;51(9):603-11.
140. Seidel H. Selected health risks caused by long-term, whole-body vibration. *Am J Ind Med*. 1993;23(4):589-604.
141. Sadani GR, Nadkarni GD. Role of tissue antioxidant defence in thyroid cancers. *Cancer Letters*. 1996;109(1-2):231-5.
142. Kim H, Lee TH, Park ES, Suh JM, Park SJ, Chung HK, et al. Role of peroxiredoxins in regulating intracellular hydrogen peroxide and hydrogen peroxide-induced apoptosis in thyroid cells. *Journal of Biological Chemistry*. 2000;275(24):18266-70.
143. Loessner D, Stok KS, Lutolf MP, Huttmacher DW, Clements JA, Rizzi SC. Bioengineered 3D platform to explore cell-ECM interactions and drug resistance of epithelial ovarian cancer cells. *Biomaterials*. 2010;31(32):8494-506.
144. Toda S, Sugihara H. Reconstruction of thyroid follicles from isolated porcine follicle cells in three-dimensional collagen gel culture. *Endocrinology*. 1990;126(4):2027-34.
145. Hong Y, Liu X, Li Z, Zhang X, Chen M, Luo Z. Real-time ultrasound elastography in the differential diagnosis of benign and malignant thyroid nodules. *J Ultrasound Med*. 2009;28(7):861-7.
146. Toda S, Koike N, Sugihara H. Thyrocyte integration, and thyroid folliculogenesis and tissue regeneration: perspective for thyroid tissue engineering. *Pathol Int*. 2001;51(6):403-17.